subcloned into HA-tagged pcDNA3 (Invitrogen). Tax construct with FLAG-tag added to the N terminus was prepared via PCR amplification of template DNA (56) with the following primers: Tax forward, 5′-CGCGAATTCATGGCCCACTTCCCAGGGTTT-3′; Tax reverse, 5′-CGCCTCGAGTCAGACTTCTGTTTCACGGAAATGTTTTTC-3′. The amplified fragment was digested with EcoRI/XhoI and subcloned into FLAG-tagged pcDNA3. The plasmid HTLV-1 provirus (pUC/HTLV-1) was provided by T. Watanabe (University of Tokyo, Tokyo, Japan) (57). A lentiviral vector, CSIICMV, was used as a null expression vector for lentiviral infection (provided by H. Miyoshi, RIKEN BioResource Center, Tsukuba, Japan) (58). CSIICMV/GFP and CSIICMV/GFP-Tax, which express GFP and GFP fused Tax, were constructed by inserting digested GFP and GFP-Tax from pEGFP (Clontech) and pEGFP-Tax, respectively, into CSIICMV.

Flow cytometric analysis. PBMCs and CSF cells were immunostained with various combinations of the following fluorescence-conjugated antibodies that tag cell surface markers: CD3 (UCHT1), CD4 (OKT4), CD25 (BC96), CCR4 (1G1), CXCR3 (1C6). In some experiments, cells were fixed with a staining buffer set (eBioscience), then intracellularly stained with antibodies against T-bet (4B10), FOXP3 (PCH101), and GATA3 (TWAJ). Cells were stained with a saturating concentration of antibody in the dark (4°C, 30 minutes) and washed twice before analysis using FACSCalibur or LSR II (BD Biosciences). Data were processed using FlowJo software (TreeStar). For cell sorting, JSAN (Bay Bioscience) was used, and the purity exceeded 95%.

Cell isolation. $CD4^+CD25^+CCR4^+$ cells, $CD4^+CD25^-CCR4^-$ cells, $CD4^+GATA3^+$ cells, and $CD4^+FOXP3^+$ cells were separated by FACS sorting. $CD4^+$ T cells were isolated from PBMCs using negative selection with magnetic beads (MACS $CD4^+$ T cell isolation kit; Miltenyi Biotec). $CD4^+CCR4^-$ or $CD4^+CCR4^+$ cells were then isolated from these $CD4^+$ T cells using positive selection with anti-CCR4 Ab (1G1) and rat anti-mouse IgG1 microbeads (Miltenyi Biotec).

Cell culture conditions. HEK293 cells were cultured in MEM (Wako Pure Chemical Industries) supplemented with 10% heat-inactivated FBS (Gibco, Invitrogen) and 1% penicillin/streptomycin (P/S) (Wako Pure Chemical Industries). HEK293T cells were cultured in DMEM-high glucose (Sigma-Aldrich) supplemented with 10% FBS and 1% P/S. Jurkat, MT-2, and JPX-9 cells were cultured in RPMI 1640 medium (Wako Pure Chemical Industries) supplemented with 10% FBS and 1% P/S. JPX-9 is a subline of Jurkat carrying Tax under the control of the metallothionein promoter (provided by M. Nakamura, Tokyo Medical and Dental University, Tokyo, Japan) (59), by which Tax expression is inducible by the addition of 20 μM $CdCl_2$ (Nacalai Tesque Inc.). PBMCs, $CD4^+CCR4^+$ cells, $CD4^+CD25^+CCR4^+$ cells, and $CD4^+CD25^-CCR4^-$ cells isolated from HDs or HAM/TSP patients were cultured in RPMI 1640 medium supplemented with 5% human AB serum (Gibco, Invitrogen) and 1% P/S.

Gene expression profiling and analyses. For transcriptional profiling, $CD4^+CD25^+CCR4^+$ T cells from a HAM/TSP patient, an ATLL patient, and an HD were separated using FACS sorting. Total RNA was prepared using ISOGEN (Nippon gene) following the manufacturer's recommendations. RNA was amplified and labeled with cyanine 3 (Cy3) using an Agilent Quick Amp Labeling Kit, 1-color (Agilent Technologies), following the manufacturer's instructions. For each hybridization, Cy3-labeled cRNA were fragmented and hybridized to an Agilent Human GE 4x44K Microarray (design ID 014850). After washing, microarrays were scanned using an Agilent DNA microarray scanner. Intensity values of each scanned feature were quantified using Agilent feature extraction software (version 9.5.3.1), which performs background subtractions. All data were analyzed using GeneSpring GX software (Agilent Technologies). There were a total of 41,000 probes on Agilent Human GE 4x44K Microarray (design ID 014850), not including control probes. Microarray data were deposited in GEO (accession no. GSE57259).

Real-time PCR and real-time RT-PCR. The HTLV-1 proviral DNA load was measured using ABI Prism 7500 SDS (Applied Biosystems) as described previously (19). For real-time RT-PCR analysis, total RNA isolation and cDNA synthesis were performed as described previously (19). Real-time PCR reactions were carried out using TaqMan Universal Master Mix (Applied Biosystems) and Universal Probe Library assays designed using ProbeFinder software (Roche Applied Science). ABI Prism 7500 SDS was programmed to have an initial step of 2 minutes at 50°C and 10 minutes at 95°C, followed by 45 cycles of 15 seconds at 95°C and 1 minute at 60°C. The primers used were as follows: *TBX21*, 5′-TGTGGTCCAAGTTTAATCAGCA-3′ (forward) and 5′-TGACAGGAATGGGAACATCC-3′ (reverse) (probe no. 9; Roche Applied Science); *Tax*, 5′-ATACAACCCCCAACATTCCA-3′ (forward) and 5′-TTTCGGAAGGGGGAGTATTT-3′ (reverse) (probe no. 69; Roche Applied Science). The primers and probes for detecting *Tax*, *IFNG*, and *GAPDH* mRNA were described previously (19). Relative quantification of mRNA was performed using the comparative Ct method using GAPDH as an endogenous control. For each sample, target gene expression was normalized to the expression of GAPDH, calculated as $2^{-(Ct[target] - Ct[GAPDH])}$.

Virus preparation and cell infection. 293T cells (1×10^6) plated in 100-mm dishes were cotransfected with the appropriate lentiviral-GFP or lentiviral-GFP-Tax expression vector (17 μg), vesicular stomatitis virus G expression vector VSV-G (pMD.G) (5 μg), rev expression vector pRSVRev (5 μg), and gag-pol expression vector pMDLg/pRRE (12 μg) (60) using Lipofectamine 2000 (Invitrogen) according to the manufacturer's protocol. After 4 hours, cells were washed 3 times with PBS, 5 ml of new medium was added, and cells were incubated for 48 hours. Culture supernatants were harvested and filtered through 0.45-μm pore size filters. Lentivirus was concentrated approximately 40-fold by low centrifugation at 6,000 *g* for 16 hours and resuspended in 2 ml RPMI 1640 medium. Freshly isolated $CD4^+CD25^+CCR4^+$ T cells were activated using Treg Suppression Inspector (Anti-Biotin MACSiBead Particles preloaded with biotinylated CD2, CD3, and CD28 antibodies) according to the manufacturer's protocol (Miltenyi Biotec). After being cultured for 36 hours, cells were transduced with equal amounts of the GFP or GFP-Tax lentivirus (MOI 15), followed by centrifugation for 1 hour at 780 *g*, 32°C. After being cultured for 4 hours at 32°C, cells were washed with culture medium and cultured in round-bottomed 96-well plates at 37°C.

Treg suppression assay. A study was conducted to compare the capacities of GFP versus GFP-Tax lentivirus–infected $CD4^+CD25^+CCR4^+$ T cells to suppress cell proliferation. T cell samples were taken from HDs, and 5×10^4 $CD4^+CD25^-$ T cells were stimulated with the Treg Suppression Inspector (see above) according to the manufacturer's instructions. These cells were then cocultured with 5×10^4 GFP lentivirus–infected $CD4^+CD25^+CCR4^+$ T cells or GFP-Tax lentivirus–infected $CD4^+CD25^+CCR4^+$ T cells. After culturing for 4 days, cell proliferation was measured using a ^3H-thymidine incorporation assay as described previously (19).

RNA interference assay. siRNA was synthesized chemically at Hokkaido System Science. The sequences of siRNA oligonucleotides were as follows: Tax, 5′-GGCCUUAUUUGGACAUUUATT-3′ and 5′-UAAAUGUCCAAAUAAGGCCTT-3′ (31); Luc, 5′-CGUACGCG-GAAUACUUCGATT-3′ and 5′-UCGAAGUAUUCCGCGUACGTT3′. Next, 100 pmol annealed RNA duplex was transfected using Human T cell Amaxa Nucleofector Kit according to the manufacturer's recommendations (Lonza). 100 pmol Luc siRNA was used as a negative control. Cells were incubated for 48 hours and then harvested and subjected to real-time RT-PCR analysis.

Measurement of IFN-γ. IFN-γ concentration in the culture supernatant was measured with a cytometric bead array kit (BD Biosciences) using a FACSCalibur flow cytometer (BD Biosciences) according to the manufacturer's instructions.

IP. Approximately 1 mg of MT-2 nuclear extracts were incubated with 5 μg anti-Tax, anti-Sp1, or normal IgG coupled with protein G–agarose (Roche Applied Science) in IP buffer (10 mM HEPES [pH 7.9], 100 mM KCl, 1 mM EDTA, 1 mM dithiothreitol, 0.1% NP-40, 1 mM Na_3VO_4, 5 mM NaF, 2 μg/ml aprotinin, 2 μg/ml leupeptin, and 2 μg/ml pepstatin) for 2 hours. The precipitated proteins were washed with the IP buffer, separated by 10% SDS-PAGE, and immunoblotted with anti-Tax or anti-Sp1 antibodies.

ChIP assay. ChIP assay was performed using a ChIP assay kit (Upstate Biotechnology) with some modifications. Briefly, 5×10^6 MT-2 cells were fixed with 1% formaldehyde at 37°C for 25 minutes and washed twice with PBS. Cells were subsequently harvested and sonicated in lysis buffer. Precleared chromatin samples were immunoprecipitated with 5 μg anti-Tax antibody, anti-Sp1 antibody, or normal IgG for 16 hours at 4°C. Immune complexes were collected with salmon sperm DNA/protein G–sepharose for 90 minutes with rotation, washed, and then incubated at 65°C for 6 hours for reverse cross-linking. Chromatin DNA was extracted and analyzed using PCR with primers for the *TBX21* promoter region (–179 to –59; forward, 5′-GCCAAGAGCGTAGAATTTGC-3′; reverse, 5′-CGCTTT-GCTGTGGCTTTATG-3′) (25, 61). Amplification was performed using ExTaq (Takara Bio) with 1 cycle at 95°C for 5 minutes followed by 30 cycles of 95°C for 30 seconds, 54°C for 30 seconds, and 72°C for 30 seconds. Amplified products were analyzed using 8% polyacrylamide gel electrophoresis.

Luciferase assay. For transient transfection, HEK293 cells were seeded at 5×10^4 cells/well into 24-well plates. After 12 hours, medium was changed to MEM supplemented with 10% FBS and 1% P/S, and each plasmid was transfected with CellPhect Transfection Kit according to the manufacturer's recommendations (GE Healthcare). 50 ng pRSV-βgal plasmid was included in each transfection experiment to control for the efficiency of transfection. The total amount of transfected DNA was kept constant with pcDNA3 in all samples. After 48 hours, cells were lysed with Passive Lysis Buffer (Promega), and luciferase activity was measured using the Promega luciferase assay system and MicroLumat Plus LB96V (Berthold Technologies). Values were normalized to β-galactosidase activity as an internal control.

Tissue staining. Formalin-fixed thoracic spinal cord tissue sections were deparaffinized in xylene and rehydrated in a series of graded alcohols and distilled water. The antigenicity of the tissue sections was recovered using a standard microwave heating technique. For immunofluorescence, the slides were incubated in PBS with 10% goat serum for 1 hour at room temperature, then in anti-CCR4 antibody, anti–T-bet antibody, anti–IFN-γ antibody, and anti-CXCR3 antibody overnight at 4°C, labeled with Alexa Fluor 488– or Alexa Fluor 594–conjugated secondary antibody, and examined under a fluorescence microscope (Nikon eclipse E600 with fluorescence filter Nikon F-FL; Nikon Instech) with rabbit or goat IgG as the negative control. Tissue sections were also stained with H&E.

Immunofluorescence staining and immunofluorescence-FISH. Jurkat cells, MT-2 cells, and cells from the CSF of 3 HAM/TSP patients were attached to slides using a cytospin centrifuge (Thermo Fisher Scientific) and fixed in 4% paraformaldehyde (Wako Pure Chemical Industries) for 30 minutes. The slides were washed with PBS and then pretreated as follows: slides were immersed in room temperature 0.2M HCl for 20 minutes, followed by 0.2% Triton-X/PBS for 10 minutes, and finally 0.005% pepsin/0.1M HCl heated to 37°C for 5 minutes. After pretreatment, the slides were stained using the immunofluorescence Can Get Signal kit (TOYOBO) according the manufacturer's instructions with anti-CCR4 as the primary antibody and Alexa Fluor 488–conjugated anti-goat IgG as the secondary antibody. After again being fixed with 4% paraformaldehyde, cells were incubated with a nick-translated (Spectrum Red) pUC/HTLV-1 DNA probe, first for 5 minutes at 70°C and then overnight at 37°C. Images were obtained under an automated research microscope (Leica DMRA2) and analyzed with CW4000 FISH software (Leica Microsystems).

Proliferation assay. PBMCs from HAM/TSP patients were plated into 96-well round-bottomed plates (1×10^5 cells/well) and cultured without any mitogenic stimuli. Cell proliferation was measured using a ^{3}H-thymidine incorporation assay as described previously (19).

Statistics. Paired 2-tailed Student's *t* test and Wilcoxon test were used for within-group comparisons. Unpaired 2-tailed Student's *t* test or Mann-Whitney *U* test was used for between-group comparisons. 1-way ANOVA was used for multiple comparisons, followed by Dunnett or Tukey test. Friedman test was used for paired multiple comparisons, followed by Dunn test. Statistical analyses were performed using Graphpad Prism 5 (GraphPad Software Inc.). A *P* value less than 0.05 was considered significant.

Study approval. Written informed consent was obtained from all patients before the study, which was reviewed and approved by the Institutional Ethics Committee at St. Marianna University and conducted in compliance with the tenets of the Declaration of Helsinki.

Acknowledgments

The authors acknowledge the excellent technical assistance provided by Yumiko Hasegawa, M. Koike, Y. Suzuki-Ishikura, and Y. Saito. This work was partly supported by project "Research on Measures for Intractable Disease"; by a matching fund subsidy from the Ministry of Health Labour and Welfare; by JSPS KAKENHI grant nos. 24790898, 25461294, and 25461293; by the Takeda Science Foundation; and by the Daiichi Sankyo Foundation of Life Science.

Address correspondence to: Yoshihisa Yamano, Department of Rare Diseases Research, Institute of Medical Science, St. Marianna University School of Medicine, 2-16-1 Sugao, Miyamae-ku, Kanagawa 216-8512, Japan. Phone: 81.44.977.8111; E-mail: yyamano@marianna-u.ac.jp.

1. Murphy KM, Stockinger B. Effector T cell plasticity: flexibility in the face of changing circumstances. *Nat Immunol*. 2010;11(8):674–680.
2. Cosmi L, Maggi L, Santarlasci V, Liotta F, Annunziato F. T helper cells plasticity in inflammation. *Cytometry A*. 2014;85(1):36–42.
3. Long SA, Buckner JH. CD4+FOXP3+ T regulatory cells in human autoimmunity: more than a numbers game. *J Immunol*. 2011;187(5):2061–2066.
4. Zhou X, Bailey-Bucktrout S, Jeker LT, Bluestone JA. Plasticity of CD4(+) FoxP3(+) T cells. *Curr Opin Immunol*. 2009;21(3):281–285.
5. Hori S, Nomura T, Sakaguchi S. Control of regulatory T cell development by the transcription factor Foxp3. *Science*. 2003;299(5609):1057–1061.
6. Zhu J, Paul WE. CD4 T cells: fates, functions, and faults. *Blood*. 2008;112(5):1557–1569.
7. Ishida T, Ueda R. Immunopathogenesis of lymphoma: focus on CCR4. *Cancer Sci*. 2011;102(1):44–50.
8. Finney OC, Riley EM, Walther M. Phenotypic analysis of human peripheral blood regulatory T cells (CD4+FOXP3+CD127lo/–) ex vivo and after in vitro restimulation with malaria antigens. *Eur J Immunol*. 2010;40(1):47–60.
9. Mjosberg J, Berg G, Jenmalm MC, Ernerudh J. FOXP3+ regulatory T cells and T helper 1, T helper 2, and T helper 17 cells in human early pregnancy decidua. *Biol Reprod*. 2010;82(4):698–705.
10. Williams LM, Rudensky AY. Maintenance of the Foxp3-dependent developmental program in mature regulatory T cells requires continued expression of Foxp3. *Nat Immunol*. 2007;8(3):277–284.
11. Bennett CL, et al. The immune dysregulation, polyendocrinopathy, enteropathy, X-linked syndrome (IPEX) is caused by mutations of FOXP3. *Nat Genet*. 2001;27(1):20–21.
12. Gao Y, et al. Molecular mechanisms underlying the regulation and functional plasticity of FOXP3(+) regulatory T cells. *Genes Immun*. 2012;13(1):1–13.
13. Dominguez-Villar M, Baecher-Allan CM, Hafler DA. Identification of T helper type 1-like, Foxp3+ regulatory T cells in human autoimmune disease. *Nat Med*. 2011;17(6):673–675.
14. Sakaguchi S, et al. Foxp3+ CD25+ CD4+ natural regulatory T cells in dominant self-tolerance and autoimmune disease. *Immunol Rev*. 2006;212:8–27.
15. Viglietta V, Baecher-Allan C, Weiner HL, Hafler DA. Loss of functional suppression by CD4+CD25+ regulatory T cells in patients with multiple sclerosis. *J Exp Med*. 2004;199(7):971–979.
16. Kanangat S, et al. Disease in the scurfy (sf) mouse is associated with overexpression of cytokine genes. *Eur J Immunol*. 1996;26(1):161–165.
17. Lyon MF, Peters J, Glenister PH, Ball S, Wright E. The scurfy mouse mutant has previously unrecognized hematological abnormalities and resembles Wiskott-Aldrich syndrome. *Proc Natl Acad Sci U S A*. 1990;87(7):2433–2437.
18. Clark LB, Appleby MW, Brunkow ME, Wilkinson JE, Ziegler SF, Ramsdell F. Cellular and molecular characterization of the scurfy mouse mutant. *J Immunol*. 1999;162(5):2546–2554.
19. Yamano Y, et al. Abnormally high levels of virus-infected IFN-γ+ CCR4+ CD4+ CD25+ T cells in a retrovirus-associated neuroinflammatory disorder. *PLoS One*. 2009;4(8):e6517.
20. Yamano Y, et al. Virus-induced dysfunction of CD4+CD25+ T cells in patients with HTLV-I-associated neuroimmunological disease. *J Clin Invest*. 2005;115(5):1361–1368.
21. Niwa R, et al. Defucosylated chimeric anti-CC chemokine receptor 4 IgG1 with enhanced antibody-dependent cellular cytotoxicity shows potent therapeutic activity to T-cell leukemia and lymphoma. *Cancer Res*. 2004;64(6):2127–2133.
22. Yoshida M, Seiki M, Yamaguchi K, Takatsuki K. Monoclonal integration of human T-cell leukemia provirus in all primary tumors of adult T-cell leukemia suggests causative role of human T-cell leukemia virus in the disease. *Proc Natl Acad Sci U S A*. 1984;81(8):2534–2537.
23. Cook LB, Rowan AG, Melamed A, Taylor GP, Bangham CR. HTLV-1-infected T cells contain a single integrated provirus in natural infection. *Blood*. 2012;120(17):3488–3490.
24. Zhang L, Zhi H, Liu M, Kuo YL, Giam CZ. Induction of p21(CIP1/WAF1) expression by human T-lymphotropic virus type 1 Tax requires transcriptional activation and mRNA stabilization. *Retrovirology*. 2009;6:35.
25. Yu J, et al. Transcriptional control of human T-BET expression: the role of Sp1. *Eur J Immunol*. 2007;37(9):2549–2561.
26. Araya N, et al. Human T-lymphotropic virus type 1 (HTLV-1) and regulatory T cells in HTLV-1-associated neuroinflammatory disease. *Viruses*. 2011;3(9):1532–1548.
27. Ando H, et al. Positive feedback loop via astrocytes causes chronic inflammation in virus-associated myelopathy. *Brain*. 2013; 136(pt 9):2876–2887.
28. Kohno T, et al. Possible origin of adult T-cell leukemia/lymphoma cells from human T lymphotropic virus type-1-infected regulatory T cells. *Cancer Sci*. 2005;96(8):527–533.
29. Satou Y, Utsunomiya A, Tanabe J, Nakagawa M, Nosaka K, Matsuoka M. HTLV-1 modulates the frequency and phenotype of FoxP3+CD4+ T cells in virus-infected individuals. *Retrovirology*. 2012;9:46.
30. Toulza F, et al. Human T-lymphotropic virus type 1-induced CC chemokine ligand 22 maintains a high frequency of functional FoxP3+ regulatory T cells. *J Immunol*. 2010;185(1):183–189.
31. Hieshima K, Nagakubo D, Nakayama T, Shirakawa AK, Jin Z, Yoshie O. Tax-inducible production of CC chemokine ligand 22 by human T cell leukemia virus type 1 (HTLV-1)-infected T cells promotes preferential transmission of HTLV-1 to CCR4-expressing CD4+ T cells. *J Immunol*. 2008;180(2):931–939.
32. Grant C, Oh U, Yao K, Yamano Y, Jacobson S. Dysregulation of TGF-β signaling and regulatory and effector T-cell function in virus-induced neuroinflammatory disease. *Blood*. 2008;111(12):5601–5609.
33. Ohsugi T, Kumasaka T. Low CD4/CD8 T-cell ratio associated with inflammatory arthropathy in human T-cell leukemia virus type I Tax transgenic mice. *PLoS One*. 2011;6(4):e18518.
34. Iwakura Y, et al. Induction of inflammatory arthropathy resembling rheumatoid arthritis in mice transgenic for HTLV-I. *Science*. 1991;253(5023):1026–1028.
35. Nakamaru Y, et al. Immunological hyperresponsiveness in HTLV-I LTR-env-pX transgenic rats: a prototype animal model for collagen vascular and HTLV-I-related inflammatory diseases. *Pathobiology*. 2001;69(1):11–18.
36. Hanon E, et al. High production of interferon gamma but not interleukin-2 by human T-lymphotropic virus type I-infected peripheral blood mononuclear cells. *Blood*. 2001;98(3):721–726.
37. Yamazato Y, Miyazato A, Kawakami K, Yara S, Kaneshima H, Saito A. High expression of p40(tax) and pro-inflammatory cytokines and chemokines in the lungs of human T-lymphotropic virus type 1-related bronchopulmonary disorders. *Chest*. 2003;124(6):2283–2292.
38. Nakamura N, et al. Human T-cell leukemia virus type 1 Tax protein induces the expression of STAT1 and STAT5 genes in T-cells. *Oncogene*. 1999;18(17):2667–2675.
39. Sun SC, Yamaoka S. Activation of NF-kappaB by HTLV-I and implications for cell transformation. *Oncogene*. 2005;24(39):5952–5964.
40. Lazarevic V, Glimcher LH. T-bet in disease. *Nat Immunol*. 2011;12(7):597–606.
41. Nishiura Y, Nakamura T, Fukushima N, Moriuchi R, Katamine S, Eguchi K. Increased mRNA expression of Th1-cytokine signaling molecules in patients with HTLV-I-associated myelopathy/tropical spastic paraparesis. *Tohoku J Exp Med*. 2004;204(4):289–298.
42. Trejo SR, Fahl WE, Ratner L. The tax protein of human T-cell leukemia virus type 1 mediates the transactivation of the c-sis/platelet-derived growth factor-B promoter through interactions with the zinc finger transcription factors Sp1 and NGFI-A/Egr-1. *J Biol Chem*. 1997;272(43):27411–27421.
43. Furuya T, et al. Heightened transmigrating activity of CD4-positive T cells through reconstituted basement membrane in patients with human T-lymphotropic virus type I-associated myelopathy. *Proc Assoc Am Physicians*. 1997; 109(3):228–236.
44. Moritoyo T, et al. Detection of human T-lymphotropic virus type I p40tax protein in cerebrospinal fluid cells from patients with human T-lymphotropic virus type I-associated myelopathy/tropical spastic paraparesis. *J Neurovirol*. 1999;5(3):241–248.
45. Umehara F, Izumo S, Ronquillo AT, Matsumuro K, Sato E, Osame M. Cytokine expression in the spinal cord lesions in HTLV-I-associated myelopathy. *J Neuropathol Exp Neurol*. 1994;53(1):72–77.
46. Matsuura E, Yamano Y, Jacobson S. Neuroimmunity of HTLV-I Infection. *J Neuroimmune Pharmacol*. 2010;5(3):310–325.
47. Nagai M, Yamano Y, Brennan MB, Mora CA, Jacobson S. Increased HTLV-I proviral load and preferential expansion of HTLV-I Tax-specific CD8+ T cells in cerebrospinal fluid from patients with HAM/TSP. *Ann Neurol*. 2001;50(6):807–812.
48. Sato T, et al. CSF CXCL10, CXCL9, and neopterin as candidate prognostic biomarkers for HTLV-1-associated myelopathy/tropical spastic paraparesis. *PLoS Negl Trop Dis*. 2013;7(10):e2479.
49. Yamamoto K, et al. Phase I study of KW-0761, a defucosylated humanized anti-CCR4 antibody, in relapsed patients with adult T-cell leukemia-lymphoma and peripheral T-cell lymphoma.

J Clin Oncol. 2010;28(9):1591–1598.
50. Ishida T, et al. Defucosylated anti-CCR4 monoclonal antibody (KW-0761) for relapsed adult T-cell leukemia-lymphoma: a multicenter phase II study. *J Clin Oncol.* 2012;30(8):837–842.
51. Yamano Y, Sato T. Clinical pathophysiology of human T-lymphotropic virus-type 1-associated myelopathy/tropical spastic paraparesis. *Front Microbiol.* 2012;3:389.
52. Yamamoto-Taguchi N, et al. HTLV-1 bZIP factor induces inflammation through labile Foxp3 expression. *PLoS Pathog.* 2013;9(9):e1003630.
53. Shimoyama M. Diagnostic criteria and classification of clinical subtypes of adult T-cell leukaemia-lymphoma. A report from the Lymphoma Study Group (1984–1987). *Br J Haematol.* 1991;79(3):428–437.
54. Osame M. Review of WHO Kagoshima meeting and diagnostic guidelines for HAM/TSP. In: Blattner W, ed. *Human Retrovirology: HTLV.* New York, New York, USA: Raven Press; 1990:191–197.
55. Tanaka Y, et al. An antigenic structure of the trans-activator protein encoded by human T-cell leukemia virus type-I (HTLV-I), as defined by a panel of monoclonal antibodies. *AIDS Res Hum Retroviruses.* 1992;8(2):227–235.
56. Yoshiki T, et al. Models of HTLV-I-induced diseases. Infectious transmission of HTLV-I in inbred rats and HTVL-I env-pX transgenic rats. *Leukemia.* 1997;11(suppl 3):245–246.
57. Kamihira S, et al. Intra- and inter-laboratory variability in human T-cell leukemia virus type-1 proviral load quantification using real-time polymerase chain reaction assays: a multi-center study. *Cancer Sci.* 2010;101(11):2361–2367.
58. Bai Y, et al. Effective transduction and stable transgene expression in human blood cells by a third-generation lentiviral vector. *Gene Ther.* 2003;10(17):1446–1457.
59. Nagata K, Ohtani K, Nakamura M, Sugamura K. Activation of endogenous c-fos proto-oncogene expression by human T-cell leukemia virus type I-encoded p40tax protein in the human T-cell line, Jurkat. *J Virol.* 1989;63(8):3220–3226.
60. Dull T, et al. A third-generation lentivirus vector with a conditional packaging system. *J Virol.* 1998;72(11):8463–8471.
61. Shin HJ, Lee JB, Park SH, Chang J, Lee CW. T-bet expression is regulated by EGR1-mediated signaling in activated T cells. *Clin Immunol.* 2009;131(3):385–394.

MAJOR ARTICLE

Mogamulizumab, an Anti-CCR4 Antibody, Targets Human T-Lymphotropic Virus Type 1–infected $CD8^+$ and $CD4^+$ T Cells to Treat Associated Myelopathy

Junji Yamauchi,[1,2] Ariella Coler-Reilly,[1] Tomoo Sato,[1] Natsumi Araya,[1] Naoko Yagishita,[1] Hitoshi Ando,[1] Yasuo Kunitomo,[1] Katsunori Takahashi,[1] Yuetsu Tanaka,[4] Yugo Shibagaki,[2] Kusuki Nishioka,[5] Toshihiro Nakajima,[5] Yasuhiro Hasegawa,[3] Atae Utsunomiya,[6] Kenjiro Kimura,[2] and Yoshihisa Yamano[1]

[1]Department of Rare Diseases Research, Institute of Medical Science, [2]Division of Nephrology and Hypertension, [3]Division of Neurology, Department of Internal Medicine, St. Marianna University School of Medicine, Kawasaki, [4]Department of Immunology, Graduate School of Medicine, University of the Ryukyus, Okinawa, [5]Institute of Medical Science, Tokyo Medical University, and [6]Department of Hematology, Imamura Bun-in Hospital, Kagoshima, Japan

Background. Human T-lymphotropic virus type 1 (HTLV-1) can cause chronic spinal cord inflammation, known as HTLV-1–associated myelopathy/tropical spastic paraparesis (HAM/TSP). Since $CD4^+CCR4^+$ T cells are the main HTLV-1 reservoir, we evaluated the defucosylated humanized anti-CCR4 antibody mogamulizumab as a treatment for HAM/TSP.

Methods. We assessed the effects of mogamulizumab on peripheral blood mononuclear cells from 11 patients with HAM/TSP. We also studied how $CD8^+$ T cells, namely $CD8^+$ $CCR4^+$ T cells and cytotoxic T lymphocytes, are involved in HTLV-1 infection and HAM/TSP pathogenesis and how they would be affected by mogamulizumab.

Results. Mogamulizumab effectively reduced the HTLV-1 proviral load (56.4% mean reduction at a minimum effective concentration of 0.01 μg/mL), spontaneous proliferation, and production of proinflammatory cytokines, including interferon γ (IFN-γ). Like $CD4^+CCR4^+$ T cells, $CD8^+CCR4^+$ T cells from patients with HAM/TSP exhibited high proviral loads and spontaneous IFN-γ production, unlike their $CCR4^-$ counterparts. $CD8^+CCR4^+$ T cells from patients with HAM/TSP contained more IFN-γ–expressing cells and fewer interleukin 4–expressing cells than those from healthy donors. Notably, Tax-specific cytotoxic T lymphocytes that may help control the HTLV-1 infection were overwhelmingly $CCR4^-$.

Conclusions. We determined that $CD8^+CCR4^+$ T cells and $CD4^+CCR4^+$ T cells are prime therapeutic targets for treating HAM/TSP and propose mogamulizumab as a new treatment.

Keywords. HTLV-1; HAM/TSP; CCR4; mogamulizumab; CD8.

Human T-lymphotropic virus type 1 (HTLV-1) infects 10–20 million people worldwide, causing HTLV-1–associated myelopathy/tropical spastic paraparesis (HAM/TSP) and adult T-cell leukemia/lymphoma (ATL) in a small fraction of infected individuals [1–3]. HAM/TSP is an inflammatory disease of the central nervous system (CNS) that is thought to develop via so-called bystander damage, meaning that the host immune responses to HTLV-1–infected cells in the CNS damage the spinal cord [4]. Currently established treatments for HAM/TSP, such as corticosteroids [5] and interferon alfa [6], do not effectively reduce the HTLV-1 proviral load, which is well correlated with disease severity [7]. Reverse transcriptase inhibitors, which are used against human immunodeficiency virus type 1, were not effective against HTLV-1 in

Received 6 May 2014; accepted 28 July 2014; electronically published 7 August 2014.

Correspondence: Yoshihisa Yamano, MD, PhD, Department of Rare Diseases Research, Institute of Medical Science, St. Marianna University School of Medicine, 2-16-1, Sugao, Miyamae-ku, Kawasaki, Kanagawa 216-8512, Japan (yyamano@marianna-u.ac.jp).

The Journal of Infectious Diseases® 2015;211:238–48

DOI: 10.1093/infdis/jiu438

clinical trials [8, 9]. These and other existing antiviral drugs usually block the viral replication process [10], but HTLV-1 may escape these drugs by replicating using host cell division [11, 12]. The ideal treatment strategy for HAM/TSP would be selectively targeting and eliminating the HTLV-1–infected cells, but no such treatments currently exist.

Mogamulizumab, a defucosylated humanized anti-CCR4 immunoglobulin G1 (IgG1) monoclonal antibody, was recently approved in Japan as a novel therapy for ATL [13]. Importantly, ATL cells usually express chemokine receptor CCR4 [14]. Mogamulizumab strongly binds to Fcγ receptor IIIa (FcγRIIIa) on natural killer (NK) cells and elicits powerful antibody-dependent cellular cytotoxicity (ADCC) against the $CCR4^+$ ATL cells [15, 16].

Recently, we found that $CD4^+CD25^+CCR4^+$ T cells are the main HTLV-1 reservoir in HAM/TSP [17]. These cells abnormally produce interferon γ (IFN-γ) and are thought to play an important role in producing the chronic inflammation in HAM/TSP [17]. Thus, we began investigating the possibility of treating HAM/TSP and ATL by targeting $CCR4^+$ cells. We have already established that the defucosylated human/mouse chimeric anti-CCR4 antibody KM2760 effectively reduces the HTLV-1 proviral load in cultured peripheral blood mononuclear cells (PBMCs) from patients with HAM/TSP [18]. Here, we evaluate for the first time the effects of the humanized antibody mogamulizumab on cells from patients with HAM/TSP.

There is a population of $CD8^+$ T cells that express CCR4, but these cells have so far received much less attention than $CD4^+$ $CCR4^+$ T cells from HTLV-1 researchers. Although it has been shown that HTLV-1 infects $CD8^+$ T cells [19], it is as of yet unknown which among $CD8^+$ T cells are predominantly infected, as well as whether and how the infection influences the functions of those cells. $CD8^+CCR4^+$ T cells are reported to suppress inflammation and play a beneficial role in controlling chronic inflammatory diseases [20, 21]. It is important to determine whether $CD8^+CCR4^+$ T cells are protective or harmful during HAM/TSP pathogenesis, as well as how these cells would be affected by mogamulizumab.

We hypothesized that $CCR4^+$ cells among $CD8^+$ and $CD4^+$ T cells are highly infected and liable to develop proinflammatory traits. It has been reported that HTLV-1 preferentially transmits to $CCR4^+$ T cells through CCL22 (a CCR4 ligand) production induced by the HTLV-1 protein product Tax [22]. Tax has also been reported to induce IFN-γ production via transcriptional alterations within the infected cells themselves [18].

In the present study, we determined that mogamulizumab is effective at reducing the proviral load and proinflammatory character in PBMCs from patients with HAM/TSP. Next, we revealed that $CD8^+CCR4^+$ T cells are indeed highly infected by HTLV-1 and become proinflammatory. Finally, we determined that the majority of Tax-specific cytotoxic T lymphocytes (CTLs) were $CCR4^-$, indicating that they would not be inadvertently targeted by mogamulizumab. Our results indicate that $CD8^+CCR4^+$ T cells should be considered a key therapeutic target when developing treatments for HAM/TSP and that mogamulizumab represents a viable candidate for such a treatment.

METHODS

Subjects

This study was approved by the Institutional Ethics Committee at St. Marianna University and conducted in compliance with the Declaration of Helsinki. All participants gave written informed consent. Blood samples were obtained from 11 patients with HAM/TSP (8 females and 3 males; median age, 57 years [range, 47–72 years]; proviral load, 4.7 copies/100 cells [range, 1.26–9.71 copies/100 cells]), 8 HTLV-1–positive asymptomatic carriers (6 females and 2 males; median age, 57 years [range, 28–76 years]; proviral load, 4.7 copies/100 cells [range, 2.43–13.19 copies/100 cells]), and 8 HTLV-1–negative healthy volunteers (6 females and 2 males; median age, 59 years [range, 51–72 years]). HTLV-1 seropositivity was determined by a particle agglutination assay (Fujirebio, Tokyo, Japan) and confirmed by Western blot (SRL Inc., Tokyo, Japan). HAM/TSP was diagnosed according to the World Health Organization guidelines [23]. PBMCs were separated by Ficoll-Hypaque density gradient centrifugation (Pancoll; PAN-Biotech, Aidenbach, Germany) and viably cryopreserved in liquid nitrogen with freezing medium (Cell Banker 1; Mitsubishi Chemical Medience Corporation, Tokyo, Japan).

Cell Culture

PBMCs were seeded at 1×10^5 cells/200 μL/well in 96-well round-bottomed plates in the presence or absence of mogamulizumab or KM2760 (gifts from Kyowa Hakko Kirin Co., Ltd., Tokyo, Japan) or human control IgG (Jackson ImmunoResearch Laboratories, West Grove, PA) or prednisolone (LKT Laboratories, Inc., St. Paul, MN) and incubated at 37°C in 5% CO_2. Roswell Park Memorial Institute 1640 medium was supplemented with 10% heat-inactivated fetal bovine serum and 1% penicillin and streptomycin antibiotic solution (Wako Pure Chemical Industries Ltd., Osaka, Japan). The supernatants were collected and stored at −80°C. The cells were harvested for DNA extraction or fluorescence-activated cell-sorter (FACS) analysis. The HTLV-1 proviral load was measured using ABI Prism 7500 SDS (Applied Biosystems, Carlsbad, CA), as described previously [24].

Cell Proliferation Assay

PBMCs from patients with HAM/TSP were cultured for 7 days as described above. PBMCs from healthy donors were stimulated with 4 μg/mL of phytohemagglutinin-P (PHA; Sigma-Aldrich, St. Louis, MO) and cultured in the presence or absence of mogamulizumab or prednisolone for 3 days. During the last 16 hours, 1 μCi of ^{3}H-thymidine was added to each well, and then cells were harvested and counted with a β-plate counter (Wallac-Perkin Elmer, Waltham, MA). The assay was performed in triplicate, and average values were used for analysis.

Measurement of Cytokines

The concentrations of 6 cytokines (IFN-γ, interleukin 2 [IL-2], interleukin 4 [IL-4], interleukin 6 [IL-6], interleukin 10 [IL-10], and tumor necrosis factor α [TNF-α]) in culture supernatants were measured with a cytometric bead array kit (BD Biosciences, San Diego, CA), using a FACSCalibur flow cytometer (BD Biosciences).

Flow Cytometric Analysis

Cells were immunostained with various combinations of the following fluorescence-conjugated antibodies to surface antigens: anti-CD3 (UCHT1), anti-CD4 (RPA-T4), anti-CD8 (RPA-T8), anti-CD14 (61D3), and anti-CD19 (HIB19), from eBiosciences (San Diego, CA); and anti-CD56 (B159) anti-CCR4 (1G1), from BD Biosciences. The epitope of the anti-CCR4 antibody (1G1) is different from that of mogamulizumab and KM2760, and thus these treatments do not affect the binding of 1G1 to CCR4 [16]. In some experiments, allophycocyanin-conjugated HLA-A*2402/HTLV-1 Tax301-309 tetramer (Medical & Biological Laboratories, Nagoya, Japan) was used. To identify HTLV-1–infected cells, cells were fixed and permeabilized using a staining buffer set (eBiosciences) and then intracellularly stained with anti-Tax antibody (Lt-4) [25]. To analyze intracellular effector molecules, cells were fixed and stained with the antibodies to perforin (δG9) and granzyme B (GB11; BD Biosciences). For intracellular cytokine staining, PBMCs were stimulated for 6 hours with phorbol 12-myristate 13-acetate (50 ng/mL) and ionomycin (1 μg/mL, Sigma-Aldrich Japan, Tokyo, Japan) in the presence of monensin (GolgiStop, BD Biosciences). After being harvested, the cells were fixed and stained with the antibodies to IFN-γ (B27) and IL-4 (MP4-25D2; BD Biosciences). The stained cells were analyzed using FACSCalibur, and the data were processed using FlowJo software (TreeStar, San Diego, CA). For cell sorting, $CD8^+$ T cells were negatively selected from PBMCs, using MACS beads (Miltenyi Biotec, Bergisch Gladbach, Germany). The purified $CD8^+$ T cells were stained with anti-CD3, anti-CD8, and anti-CCR4 antibodies, and then $CD3^+CD8^+$, $CD3^+CD8^+CCR4^+$, and $CD3^+CD8^+CCR4^-$ T cells were separated using a cell sorter (JSAN, Bay Bioscience Co., Ltd., Hyogo, Japan). The purity exceeded 95%.

Statistical Analysis

Values are expressed as means ± standard deviations. The paired *t* test or the Wilcoxon signed-rank test was used for within-group comparisons. The Mann–Whitney *U* test was used for comparisons between groups. Repeated-measures analysis of variance (ANOVA) followed by the Dunnett test or the Friedman test followed by the Dunn test were used for paired multiple comparisons. Statistical analyses were performed using GraphPad Prism 5 and Prism statistics (GraphPad Software, Inc., La Jolla, CA), and *P* values of <.05 were considered statistically significant.

RESULTS

Mogamulizumab and KM2760 Reduce the HTLV-1 Proviral Load and Inhibit Spontaneous Proliferation of PBMCs From Patients With HAM/TSP

The effects of mogamulizumab and KM2760 were assessed by measuring proviral loads in treated PBMCs from patients with HAM/TSP. ^{3}H-thymidine incorporation was used to assess the inhibitory effects of the antibodies on spontaneous cell proliferation, a distinctive phenomenon associated with PBMCs from HTLV-1–infected individuals by which the cells proliferate without mitogens or stimuli in vitro [26]. Mogamulizumab and KM2760 both reduced proviral load in a dose-dependent manner at concentrations of ≥0.01 μg/mL (mean reduction [±SD], 56.4% ± 21.1% and 61.1% ± 17.0%, respectively; $P < .01$ and $P < .001$, respectively; Figure 1*A*). Notably, there was a mean reduction (±SD) of 66.4% ± 20.2% in the proviral load with 10 μg/mL mogamulizumab ($P < .001$), which is the blood concentration of the antibody in patients with ATL treated with 1 mg/kg mogamulizumab [13]. Mogamulizumab and KM2760 similarly inhibited spontaneous proliferation in a dose-dependent manner at concentrations of ≥0.01 μg/mL (mean inhibition [±SD], 25.6% ± 31.9% and 22.1% ± 35.9%, respectively; $P < .01$ and $P < .05$, respectively; Figure 1*B*). Because mogamulizumab and KM2760 showed such similar results, only mogamulizumab was used in the next experiments as representative of the 2. Mogamulizumab was also tested against human IgG to control for nonspecific antibody effects and more effectively reduced the proviral load and spontaneous proliferation (Supplementary Figure 1*A* and 1*B*). Mogamulizumab reduced the HTLV-1 proviral load in cells from asymptomatic carriers, as well, in a dose-dependent manner (Figure 1*C*). Finally, mogamulizumab inhibited PHA-stimulated proliferation of PBMCs from healthy donors at concentrations of ≥0.1 μg/mL ($P < .01$), but the effects of prednisolone were much more pronounced than those of mogamulizumab (prednisolone vs mogamulizumab, $P < .001$; Figure 1*D*).

Prednisolone suppressed spontaneous proliferation (mean inhibition [±SD], 37.4% ± 35.2%; $P < .001$; Figure 1*B*) but did not decrease proviral load (Figure 1*A*). The combination of mogamulizumab and 0.1 μg/mL of prednisolone, which corresponds to the serum concentration achieved when 5 mg of prednisolone is administered orally [27], reduced proviral load as much as but no more than did mogamulizumab alone (Supplementary Figure 2*A*). On the other hand, ^{3}H-thymidine incorporation was substantially more inhibited by the combination treatment than with mogamulizumab alone (mean inhibition [±SD], 81.3% ± 18.3% vs 71.3% ± 19.3%; $P = .01$; Supplementary Figure 2*B*).

Mogamulizumab and KM2760 Inhibit Proinflammatory Cytokine Production in PBMCs From HAM/TSP Patients

Here we examined the effects of mogamulizumab and KM2760 on cytokine production in PBMCs from patients with HAM/

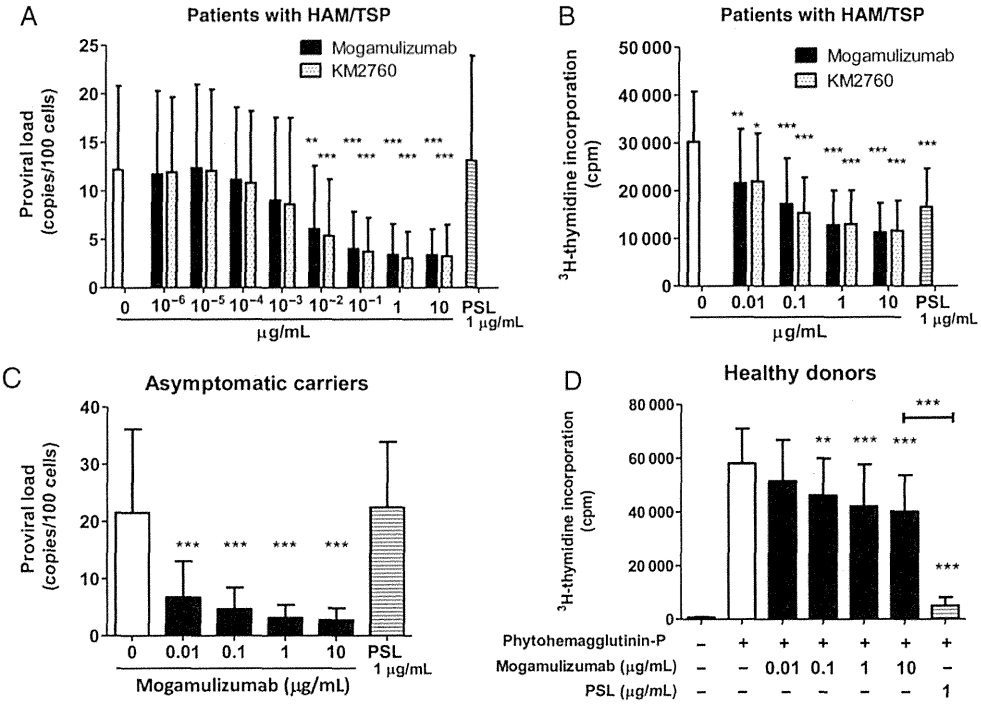

Figure 1. Mogamulizumab and KM2760 reduce the human T-lymphotropic virus type 1 (HTLV-1) proviral load and inhibit spontaneous proliferation of peripheral blood mononuclear cells (PBMCs) from patients with HTLV-1–associated myelopathy/tropical spastic paraparesis (HAM/TSP). *A* and *B*, PBMCs from 11 patients with HAM/TSP were cultured for 7 days without stimuli and without treatment or in the presence of mogamulizumab, KM2760, or prednisolone (PSL). Cells were harvested, and the proviral load was measured using real-time polymerase chain reaction (*A*). ^{3}H-thymidine was added during the last 16 hours of culturing. Cells were then harvested and analyzed for ^{3}H-thymidine incorporation (*B*). Because mogamulizumab and KM2760 were equally effective, only mogamulizumab was used thereafter as representative of the 2. *C*, PBMCs from 8 asymptomatic carriers were cultured for 7 days without treatment or in the presence of mogamulizumab or PSL, and the proviral load was measured as described above. *D*, PBMCs from 8 healthy donors were stimulated with 4 μg/mL of phytohemagglutinin-P and cultured for 3 days without treatment or in the presence of mogamulizumab or PSL. ^{3}H-thymidine incorporation was analyzed as described above. Data are presented as the mean ± SD. Statistical analyses were performed using repeated-measures analysis of variance, followed by the Dunnett test, for comparison with PBMCs alone (*A–C*) or with PBMCs stimulated with PHA (*D*). The paired *t* test was used to compare 10 μg/mL of mogamulizumab and PSL (*D*). **P* < .05, ***P* < .01, and ****P* < .001. Abbreviation: SD, standard deviation.

TSP. In line with previous reports [28], PBMCs produced various cytokines, most notably IFN-γ, in 7-day cultures without stimuli (Figure 2*A*). Mogamulizumab and KM2760 both reduced the production of the proinflammatory cytokines IFN-γ, IL-6, IL-2, and TNF-α, as well as the immunosuppressive cytokine IL-10 (Figure 2*B–F*). Mogamulizumab reduced IFN-γ production more than did human IgG (Supplementary Figure 1*C*). Prednisolone at a concentration of 1 μg/mL effectively reduced IFN-γ and TNF-α but not IL-2, IL-6, or IL-10 production.

Mogamulizumab Eliminates CCR4^{+} Cells Among Both CD4^{+} and CD8^{+} T cells

Mogamulizumab effectively eliminated the CD4^{+}CCR4^{+} T cells in cultured PBMCs from patients with HAM/TSP (Figure 3*A* and 3*B*). FACS analysis also revealed a population of CD4^{-} CCR4^{+} cells similarly affected by the antibody, and these cells were found to be CD8^{+} T cells (Figure 3*C*). Detailed investigation confirmed that CCR4^{+} T cells among the CD8^{+} subset were eliminated by mogamulizumab just as they were from the CD4^{+} subset (Figure 3*D–E*).

The ADCC Activity of Mogamulizumab Is Fast Acting and Specific

FACS analysis showed that mogamulizumab reduced the frequency of CCR4^{+} T cells among both CD4^{+} and CD8^{+} subsets within 6 hours ($P = .0003$ and $P = .004$, respectively), with a similar reduction in Tax^{+} T cells observed within 24 hours ($P = .01$ and $P = .03$, respectively; Figure 4*A–C* and Supplementary Figure 3). By contrast, mogamulizumab did not reduce the frequency of B cells, NK cells, or monocytes after 24 hours (Figure 4*D*).

CD8^{+}CCR4^{+} T Cells From Patients With HAM/TSP Are Numerous and Highly Infected by HTLV-1

CD8^{+}CCR4^{+} T cells were then further analyzed to assess their role in HAM/TSP and predict the potential benefits and risks of eradicating them with mogamulizumab. Samples from patients with HAM/TSP, compared with those from age-matched healthy donors, contained a higher proportion of CCR4^{+} cells among both the CD4^{+} T-cell subset ($P = .003$) and the CD8^{+} T-cell subset ($P = .02$; Figure 5*A*). In addition, the proviral

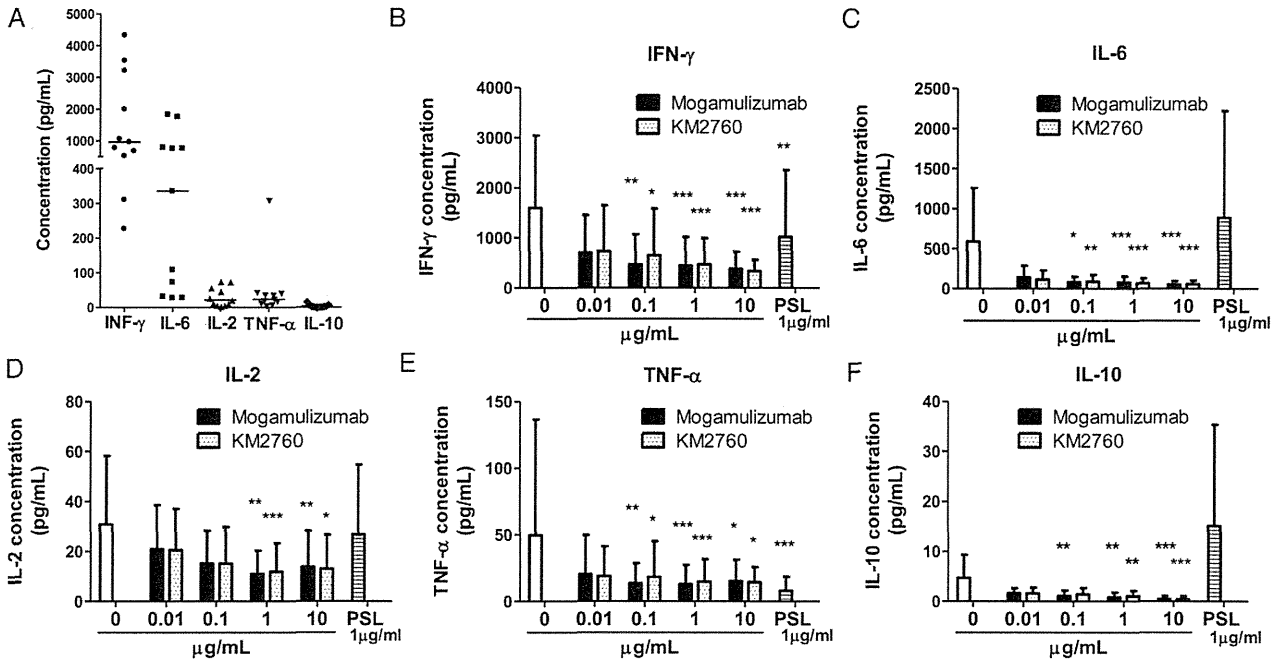

Figure 2. Mogamulizumab and KM2760 inhibit cytokine production in peripheral blood mononuclear cells (PBMCs) from patients with human T-lymphotropic virus type 1–associated myelopathy/tropical spastic paraparesis (HAM/TSP). PBMCs from 11 patients with HAM/TSP were cultured for 7 days without stimuli and without treatment or in the presence of mogamulizumab, KM2760, or prednisolone (PSL). The concentrations of cytokines (interferon γ [IFN-γ], interleukin 6 [IL-6], interleukin 2 [IL-2], tumor necrosis factor α [TNF-α], and interleukin 10 [IL-10]) in the supernatants were then measured. *A*, Direct comparison of the concentrations of these cytokines in the supernatants of untreated PBMC cultures. Horizontal bars represent the median values. *B–F*, The effects of the treatments on the concentrations of these cytokines. Data are presented as the mean ± SD. Statistical analyses were performed using the Friedman test followed by the Dunn test for comparison with PBMCs alone. $^{*}P < .05$, $^{**}P < .01$, and $^{***}P < .001$. Abbreviation: SD, standard deviation.

load was significantly higher in $CD8^+CCR4^+$ T cells than in $CD8^+CCR4^-$ T cells (mean load [±SD], 13.6 ± 7.9 copies/100 cells and 0.72 ± 0.65 copies/100 cells, respectively; $P = .0002$; Figure 5*B*).

$CD8^+CCR4^+$ T Cells From Patients With HAM/TSP Possess Proinflammatory Properties

Here we investigated the functional differences between $CD8^+CCR4^+$ T cells from patients with HAM/TSP and those from healthy donors. $CD8^+CCR4^+$ cells from both groups expressed minimal perforin and granzyme B (Figure 5*C* and 5*D*). In the $CD8^+CCR4^-$ T-cell subset, the frequency of perforin-expressing cells was unremarkable, but the frequency of granzyme B–expressing cells was higher in patients with HAM/TSP than in healthy donors ($P = .04$; Figure 5*C* and 5*D*). Next, cytokine expression was evaluated in PBMCs stimulated with phorbol 12-myristate 13-acetate and ionomycin in the presence of monensin. Interestingly, samples from patients with HAM/TSP included more IFN-γ–producing cells ($P = .02$; Figure 5*E*) but fewer IL-4–producing cells ($P = .01$; Figure 5*F*) in the $CD8^+CCR4^+$ T-cell subset than did samples from healthy donors. On the other hand, there were no such significant differences among $CD8^+CCR4^-$ T cells (Figure 5*E* and 5*F*).

Finally, the concentrations of cytokines in the supernatants of unstimulated cultures of isolated total $CD8^+$, $CD8^+CCR4^-$, and $CD8^+CCR4^+$ T cells were measured to assess spontaneous cytokine production in these cell populations. Spontaneous IFN-γ production, like spontaneous proliferation, is a hallmark of PBMCs from patients with HAM/TSP [29,30]. Unsurprisingly, IFN-γ was detected in no cell population from healthy donors. Among samples from patients with HAM/TSP, $CD8^+CCR4^+$ T cells produced remarkably more IFN-γ than did $CD8^+CCR4^-$ cells (mean level [±SD], 364.0 ± 445.3 pg/mL vs 1.9 ± 4.5 pg/mL; $P = .001$; Figure 5*G*). IL-4 was not detected in any of the samples (data not shown).

The Majority of HTLV-1 Tax-Specific Cytotoxic T Lymphocytes Are $CCR4^-$

We analyzed CCR4 expression in Tax-specific CTLs to determine whether CTLs against HTLV-1 also become targets of mogamulizumab. Among the 11 patients studied, 7 had HLA-A*2402 and were analyzed using the HLA-A*2402/HTLV-1 Tax301-309 tetramer. The majority of Tax-specific CTLs did not express CCR4, and the percentage of $CCR4^+$ cells was lower in CTLs than in total $CD8^+$ T cells (mean frequency [±SD], 2.3% ± 1.0% and 8.5 ± 4.7%, respectively; $P = .02$; Figure 6).

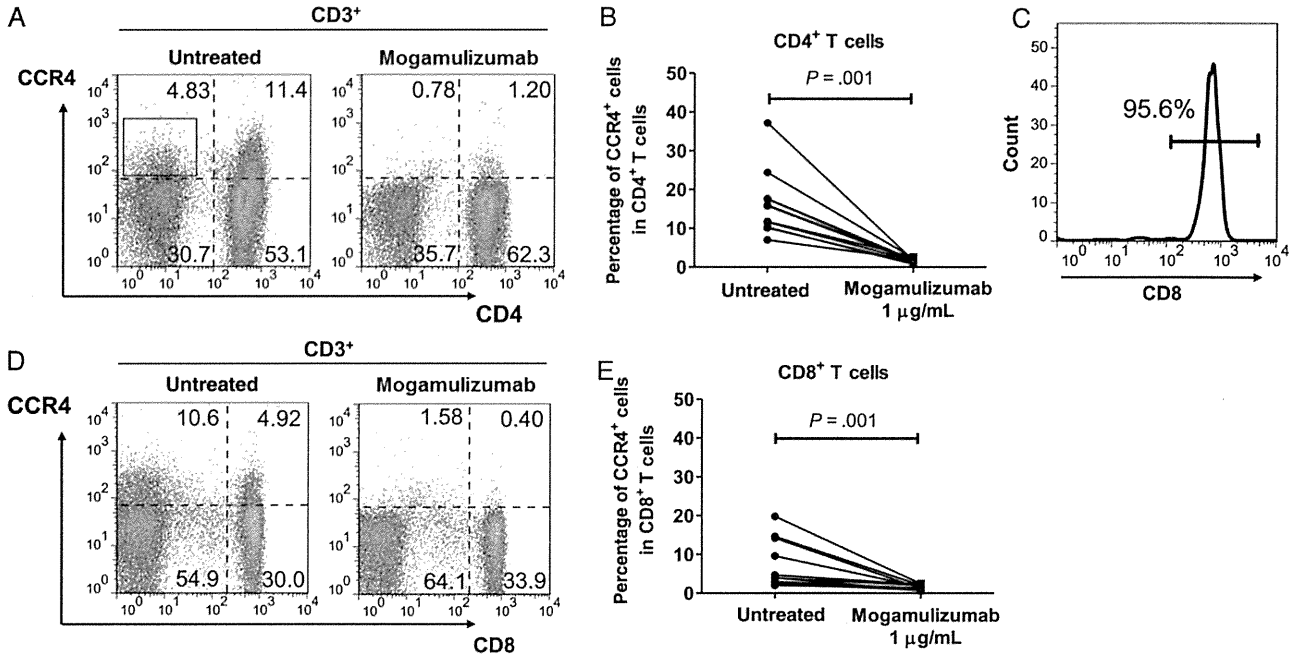

Figure 3. Mogamulizumab eliminates $CCR4^+$ cells in both $CD4^+$ and $CD8^+$ T cells. *A*, Representative dot plots of fluorescence-activated cell-sorter analysis of CCR4 and CD4 expression in $CD3^+$ T cells among peripheral blood mononuclear cells from patients with human T-lymphotropic virus type 1–associated myelopathy/tropical spastic paraparesis after 5-day culture in the presence or absence of 1 μg/mL of mogamulizumab. *B*, Percentages of $CCR4^+$ cells in $CD3^+CD4^+$ T cells were compared between the untreated and mogamulizumab groups (n = 11). Statistical analysis was performed using the Wilcoxon signed-rank test. *C*, The population enclosed in the box in panel *A* (the $CD3^+CD4^-CCR4^+$ subset) was gated and analyzed for the expression of CD8. The percentage of $CD8^+$ cells is shown. *D* and *E*, CCR4 and CD8 expression in $CD3^+$ T cells was analyzed as described above.

DISCUSSION

In this study, we established mogamulizumab as a novel candidate treatment for HAM/TSP that targets infected cells by marking $CCR4^+$ T cells for elimination. Mogamulizumab reduced the number of infected cells, as measured via the proviral load, and thus inhibited the excessive immune responses such as spontaneous proliferation and proinflammatory cytokine production that are attributed to those infected cells (Figures 1 and 2). Effects of mogamulizumab-induced ADCC activity were detectable by FACS after as little as 6 hours of culturing (Figure 4*A*–*C*).

The remaining proviral load after mogamulizumab therapy was higher than expected (mean load [±SD], 3.25 ± 2.58 copies/100 cells; Figure 1*A*). $CD4^+CCR4^-$ T cells [18] and $CD8^+CCR4^-$ T cells (Figure 5*B*) from patients with HAM/TSP were predominantly uninfected, and the antibody therapy should have destroyed the vast majority of the infected $CCR4^+$ T cells (Figure 3), yielding an expected proviral load of <1.0 copy/100 cells. It is possible that some $CCR4^-$ T cells became infected while the samples were being cultured, which is a potential limitation of such in vitro experiments.

The inhibitory effects of mogamulizumab on PHA-stimulated proliferation in PBMCs from healthy donors were statistically significant but still minimal, compared with those of prednisolone (Figure 1*D*), indicating that mogamulizumab, in contrast to immunosuppressive agents, acts via specific reduction of infected cells rather than via nonspecific immune suppression. Interestingly, prednisolone was considerably less effective at suppressing the proliferation of T cells from patients with HAM/TSP (Figure 1*B*) than from healthy donors. Although we cannot be sure of the reasons behind this discrimination, it appears that spontaneous proliferation is less vulnerable to suppression by steroids since it is not a simple T-cell response to antigens [31, 32]. Nevertheless, compared with mogamulizumab alone, the combination with prednisolone enhanced the suppressive effect of mogamulizumab on spontaneous proliferation without hampering proviral load reduction (Supplementary Figure 2).

Mogamulizumab also reduced the proviral load in PBMCs from asymptomatic carriers (Figure 1*C*), which suggests that it can be administered as a preventive treatment to asymptomatic carriers with high proviral loads who are at risk for developing HAM/TSP or ATL. It is well established that high proviral load is associated with the onset and progression of HAM/TSP [7, 33], as well as with the development of ATL [34].

It was well known that although the main reservoir for HTLV-1 is $CD4^+$ T cells, the virus also infects $CD8^+$ T cells in patients

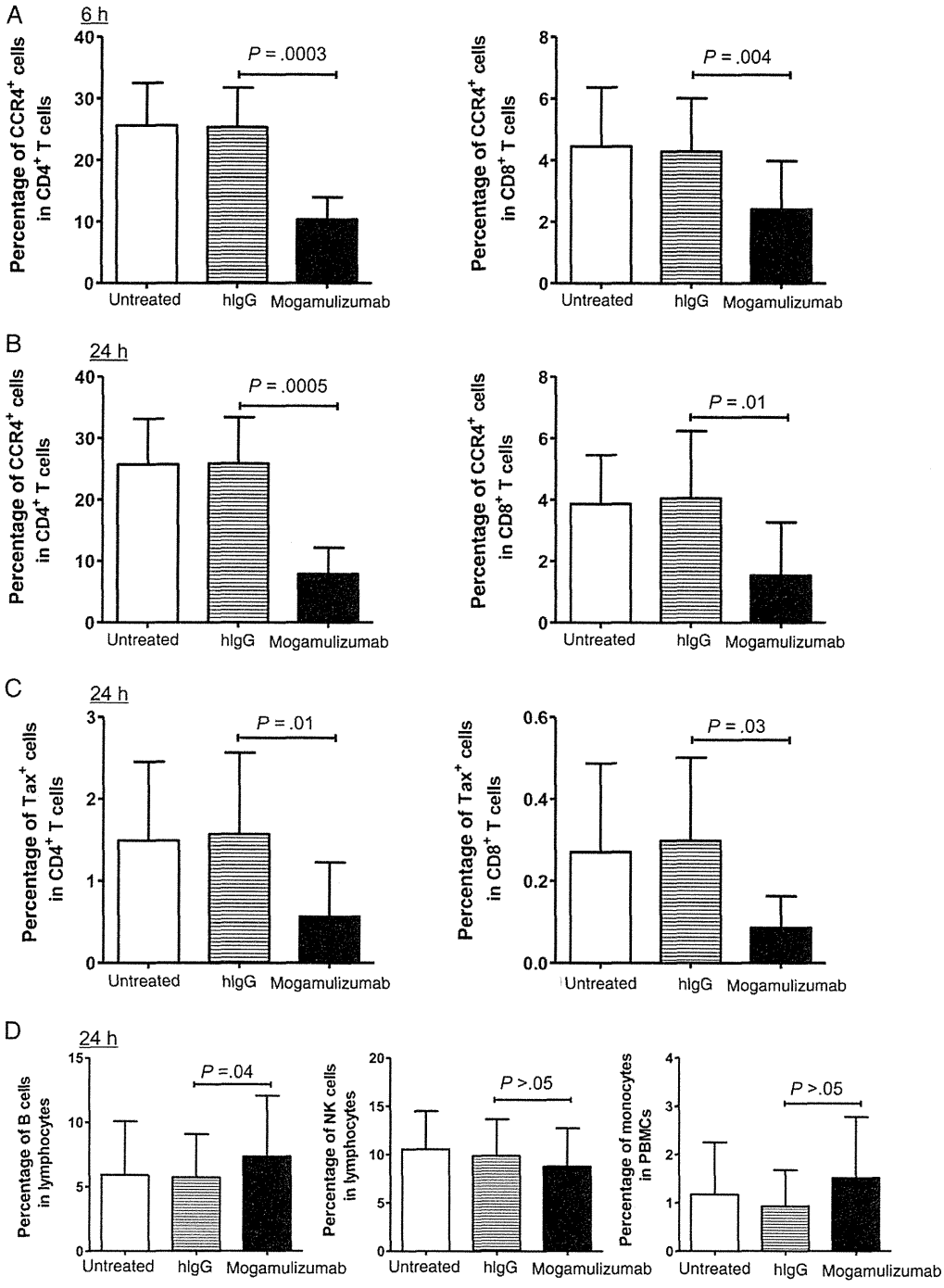

Figure 4. The antibody-dependent cellular cytotoxicity activity of mogamulizumab is fast acting and specific. Peripheral blood mononuclear cells (PBMCs) from 6 patients with human T-lymphotropic virus type–associated myelopathy/tropical spastic paraparesis were cultured in the presence of 1 μg/mL of mogamulizumab or human immunoglobulin G (hIgG) or without treatment. $CD4^+$ and $CD8^+$ T cells were analyzed using fluorescence-activated cell-sorter analysis, and the frequencies of $CCR4^+$ cells after 6 hours (*A*) and 24 hours (*B*), as well as that of Tax^+ cells (*C*) after 24 hours, are shown here. The frequencies of $CD19^+$ B cells and $CD3^-CD56^+$ natural killer (NK) cells among lymphocytes, as well as $CD14^+$ monocytes among PBMCs after 24 hours are also shown (*D*). Data are presented as the mean ± SD. The paired *t* test was used to compare the effects of mogamulizumab and hIgG. Abbreviation: SD, standard deviation.

with HAM/TSP [19]. Here we revealed for the first time that the overwhelming majority of infected $CD8^+$ T cells also expressed CCR4 (Figure 5*B*). Our findings in this study suggest that it is important to eliminate both $CD4^+CCR4^+$ and $CD8^+CCR4^+$ T-cell subsets because both have elevated proviral loads and a tendency to develop proinflammatory traits (Figure 5).

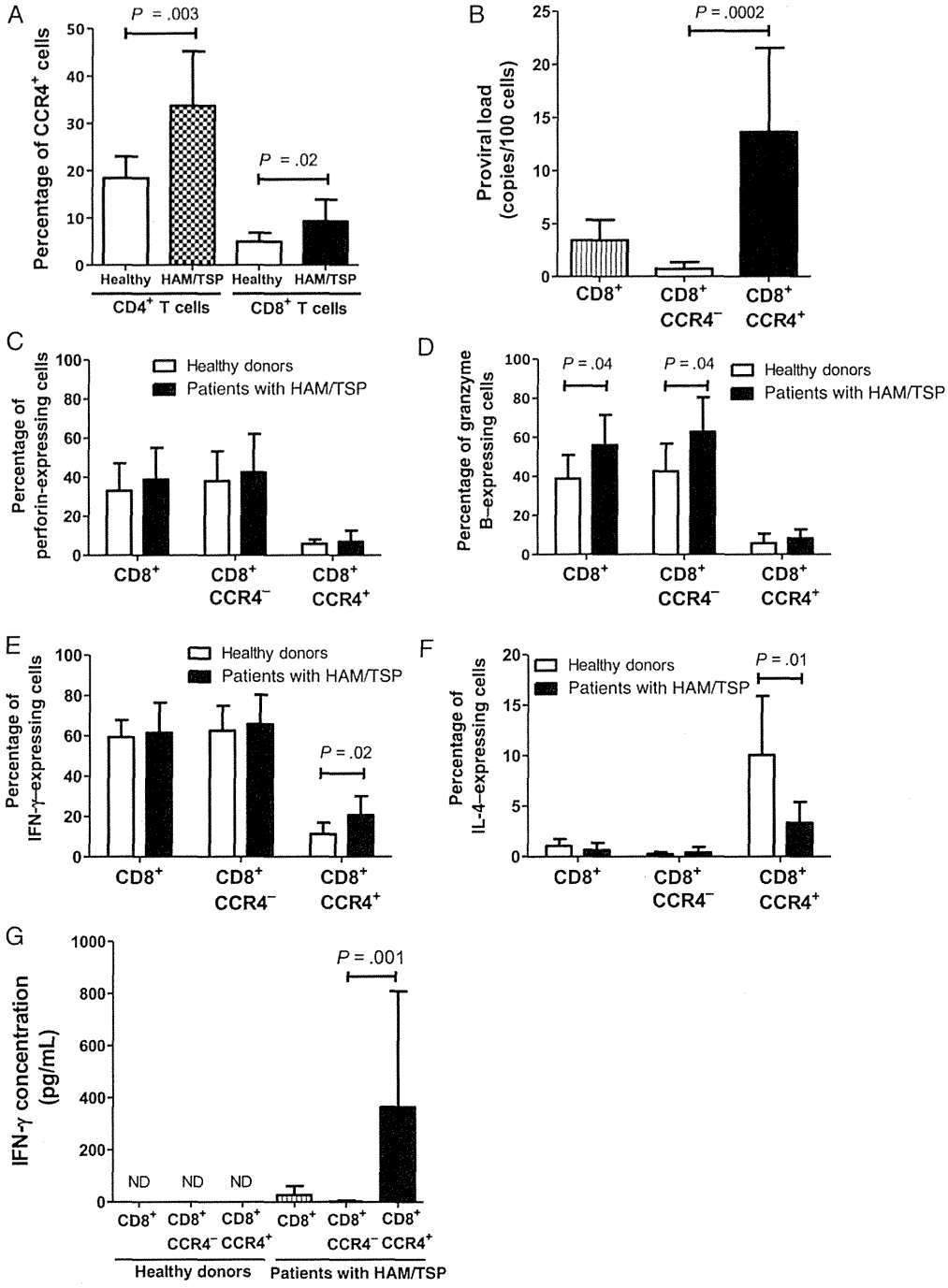

Figure 5. $CD8^+CCR4^+$ T cells from patients with human T-lymphotropic virus type 1 (HTLV-1)–associated myelopathy/tropical spastic paraparesis (HAM/TSP) are numerous, highly HTLV-1 infected, and proinflammatory. *A*, Proportions of $CCR4^+$ cells among $CD4^+$ and $CD8^+$ T cells in 8 healthy donors and 11 patients with HAM/TSP were analyzed by fluorescence-activated cell-sorter (FACS) analysis. *B*, The HTLV-1 proviral load in total $CD3^+CD8^+$, $CD3^+CD8^+CCR4^-$, and $CD3^+CD8^+CCR4^+$ T-cell subsets. $CD8^+$ T cells from 11 patients with HAM/TSP were isolated using negative separation with magnetic beads, and then $CD3^+CD8^+$, $CD3^+CD8^+CCR4^-$ and $CD3^+CD8^+CCR4^+$ T cells were separated with FACS analysis. Proviral loads in each subset were measured using real-time polymerase chain reaction. *C–F*, Peripheral blood mononuclear cells (PBMCs) from 8 healthy donors and 11 patients with HAM/TSP were stained for CD8 and CCR4, as well as intracellular perforin or granzyme B, and analyzed using FACS analysis. PBMCs from the same individuals were stimulated with phorbol 12-myristate 13-acetate (50 ng/mL) and ionomycin (1 μg/mL) in the presence of monensin for 6 hours. The cells were then analyzed for CD8, CCR4, and intracellular interferon γ (IFN-γ) or interleukin 4 (IL-4) expressions. The percentages of perforin-expressing (*C*), granzyme B–expressing (*D*), IFN-γ–expressing (*E*), and IL-4–expressing (*F*) cells in total $CD8^+$, $CD8^+CCR4^-$, and $CD8^+CCR4^+$ T-cell subsets from healthy donors versus patients with HAM/TSP are shown. *P* values are indicated only when <.05. *G*, $CD3^+CD8^+$, $CD3^+CD8^+CCR4^-$, and $CD3^+CD8^+CCR4^+$ T cells were isolated from 6 healthy donors and 11 patients with HAM/TSP as described above. These cells (3×10^4 cells/well) were cultured for 3 days without stimuli, and the concentration of IFN-γ in the supernatants was measured. Statistical analysis was performed using the Mann–Whitney *U*-test (*A* and *C–F*) or the Wilcoxon signed-rank test (*B* and *G*). Data are presented as the mean ± SD. Abbreviation: SD, standard deviation.

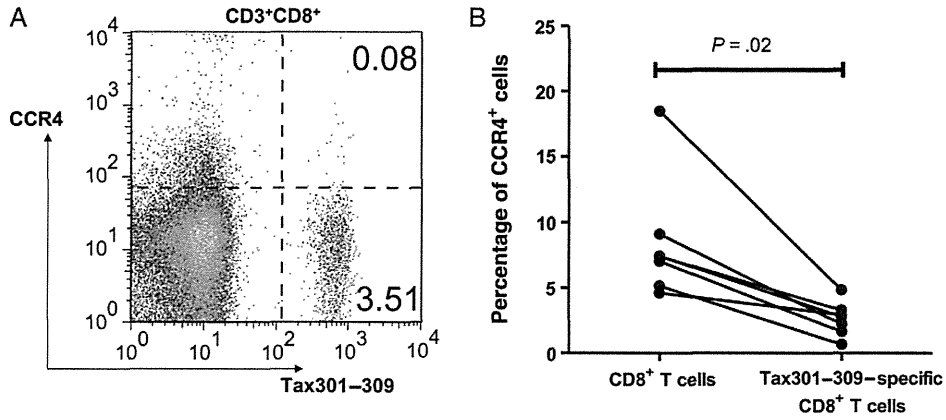

Figure 6. $CD8^+CCR4^+$ T cells from patients with human T-lymphotropic virus type 1 (HTLV-1)–associated myelopathy/tropical spastic paraparesis (HAM/TSP) do not include many Tax-specific cytotoxic T lymphocytes (CTLs). *A*, A representative dot plot of fluorescence-activated cell-sorter (FACS) analysis of the expression of CCR4 in HTLV-1 Tax-specific CTLs. Peripheral blood mononuclear cells from a patient with HAM/TSP and HLA-A*2402 were stained with antibodies for CD3, CD8, CCR4, and HLA-A*2402-restricted Tax301-309–specific tetramer. The $CD3^+CD8^+$ subset was gated. The values in the upper and lower right quadrants indicate the percentages of $CCR4^+$ and $CCR4^-$ Tax-specific CTLs among $CD3^+CD8^+$ T cells, respectively. *B*, Proportions of $CCR4^+$ cells among total $CD8^+$ T cells and Tax301-309–specific $CD8^+$ T cells are compared (n = 7). Statistical analysis was performed using the Wilcoxon signed-rank test.

$CD8^+CCR4^+$ T cells normally produce IL-4 more often than IFN-γ and hardly produce any cytotoxic granules [35, 36]; these cells are thought to be protective against type 1-skewed inflammation [21, 37]. In patients with HAM/TSP, these $CD8^+CCR4^+$ but not $CD8^+CCR4^-$ T cells are altered to produce IFN-γ rather than IL-4 (Figure 5*E* and 5*F*). $CD8^+CCR4^+$ T cells cultured alone exhibited spontaneous IFN-γ production (Figure 5*G*), a hallmark of PBMCs from patients with HAM/TSP [29, 30]. These results suggest that abnormal cells contributing to the pathogenesis of HAM/TSP exist not only among $CD4^+CCR4^+$ T cells but also among $CD8^+CCR4^+$ T cells. It is thought that the functional abnormalities of these cells may arise through transformations occurring within the infected cells themselves, whereby HTLV-1 Tax induces transcriptional alterations via T box transcription factor [18].

In the present study, HTLV-1 infection did not influence cytotoxic granule production in $CD8^+CCR4^+$ T cells (Figure 5*C* and 5*D*). The slightly increased fraction of granzyme B^+ cells in $CD8^+CCR4^-$ T cells from patients with HAM/TSP is presumably attributable to the immune activation resulting from the chronic viral infection [38–40].

Although eliminating the abnormal immune responses of the infected cells should alleviate inflammation and related symptoms of the infection, it is also true that immune responses against HTLV-1 are important for controlling said infection [41]. We evaluated CCR4 expression in HTLV-1 Tax-specific CTLs for fear that use of mogamulizumab might inadvertently destroy CTLs that would have helped to control the infection [42, 43]. Since Tax-specific CTLs have been reported to be preferentially infected by HTLV-1 [44], there was some concern that our finding that infected $CD8^+$ T cells are predominantly $CCR4^+$ meant that these CTLs would also be targeted by mogamulizumab. However, we found that the majority of Tax-specific CTLs do not express CCR4 (Figure 6), meaning that they should essentially be spared during mogamulizumab treatment.

Also concerning is that mogamulizumab is expected to target $CD4^+CCR4^+$ regulatory T (Treg) cells [45], which could elicit autoimmune problems and even exacerbate the chronic inflammation plaguing patients with HAM/TSP. However, there are also $CCR4^-$ Treg cells [45], which would be spared, and there have been no reports of increased incidence of autoimmune disease in patients with ATL treated with mogamulizumab. Furthermore, reducing the number of Treg cells may benefit patients with HAM/TSP by preventing abundant Treg cells from dampening immune control of the HTLV-1 infection [28, 46].

We expect that eliminating HTLV-1–infected cells in the peripheral blood with mogamulizumab would reduce the number of proinflammatory cells and mitigate the inflammation in the CNS. Although HAM/TSP is a disease of the CNS, recent reports suggest that it is indeed effective to target HTLV-1–infected cells in the peripheral blood because continued migration of infected cells from the peripheral blood maintains and even exacerbates the inflammation in the CNS [30].

Based on the results of this study, we have begun conducting a clinical trial to test the efficacy of mogamulizumab on patients with HAM/TSP (UMIN000012655). Our data suggest that as little as one thousandth of the dose administered to patients with ATL (1 mg/kg body weight [13]) may be effective for patients with HAM/TSP. In contrast to patients with an aggressive cancer such as ATL, those with a chronic inflammatory disorder like HAM/TSP would benefit from a more conservative approach that is safer but still effective.

In conclusion, we have demonstrated that mogamulizumab shows promise as a novel treatment for HAM/TSP. Our results indicate that $CD8^+CCR4^+$ T cells and $CD4^+CCR4^+$ T cells are key therapeutic targets and, thus, that the CCR4-targeting therapy mogamulizumab can be expected to effectively ameliorate chronic inflammation in patients with HAM/TSP. The lack of success with classic antiviral therapies [8, 9] suggests that blocking viral replication is ineffective against HTLV-1, which mainly spreads by cell division [11, 12]. Targeting the infected cells themselves on the basis of their characteristic markers may be the key to combating this tricky virus. If successful, mogamulizumab would become the first treatment for a chronic viral infection that effectively targets infected cells.

Supplementary Data

Supplementary materials are available at *The Journal of Infectious Diseases* online (http://jid.oxfordjournals.org). Supplementary materials consist of data provided by the author that are published to benefit the reader. The posted materials are not copyedited. The contents of all supplementary data are the sole responsibility of the authors. Questions or messages regarding errors should be addressed to the author.

Notes

Acknowledgments. We thank M. Koike, Y. Hasegawa, Y. Suzuki-Ishikura, and Y. Saito, for technical assistance; and Kyowa Hakko Kirin, Japan, for kindly providing monoclonal antibodies (mogamulizumab and KM2760).

J. Y. performed most of the experiments, performed data analysis, created the figures, and wrote the manuscript. A. C. R. performed data interpretation and wrote the manuscript. T. S., N. A., N. Y., H. A., Y. K., and K. T. performed data analysis and interpretation. Y. T., Y. S., K. N., T. N., Y. H., A. U., and K. K. reviewed and edited the manuscript. Y. Y. developed the project, performed data analysis, and wrote the manuscript. All authors approved the final manuscript.

Financial support. This work was supported by the Ministry of Health Labor and Welfare (matching-fund subsidy for the Research on Measures for Intractable Disease project), JSPS KAKENHI (grant 25461294), and the MEXT-Supported Program for the Strategic Research Foundation at Private Universities, 2008–2012.

Potential conflicts of interest. Y. Y. has 1 established patent and another pending for the use of anti-CCR4 antibodies as a treatment for HAM/TSP. All other authors report no potential conflicts.

All authors have submitted the ICMJE Form for Disclosure of Potential Conflicts of Interest. Conflicts that the editors consider relevant to the content of the manuscript have been disclosed.

References

1. Gessain A, Barin F, Vernant JC. Antibodies to human T-lymphotropic virus type-I in patients with tropical spastic paraparesis. Lancet **1985**; 2:407–10.
2. Osame M, Usuku K, Izumo S, et al. HTLV-I associated myelopathy, a new clinical entity. Lancet **1986**; 1:1031–2.
3. Verdonck K, González E, Van Dooren S, Vandamme A, Vanham G, Gotuzzo E. Human T-lymphotropic virus 1: recent knowledge about an ancient infection. Lancet Infect Dis **2007**; 7:266–81.
4. Ijichi S, Izumo S, Eiraku N, et al. An autoaggressive process against bystander tissues in HTLV-I-infected individuals: a possible pathomechanism of HAM/TSP. Med Hypotheses **1993**; 41:542–7.
5. Nakagawa M, Nakahara K, Maruyama Y, et al. Therapeutic trials in 200 patients with HTLV-I-associated myelopathy/tropical spastic paraparesis. J Neurovirol **1996**; 2:345–55.
6. Izumo S, Goto I, Itoyama Y, et al. Interferon-alpha is effective in HTLV-I-associated myelopathy: a multicenter, randomized, double-blind, controlled trial. Neurology **1996**; 46:1016–21.
7. Olindo S, Lézin A, Cabre P, et al. HTLV-1 proviral load in peripheral blood mononuclear cells quantified in 100 HAM/TSP patients: a marker of disease progression. J Neurol Sci **2005**; 237:53–9.
8. Taylor GP, Goon P, Furukawa Y, et al. Zidovudine plus lamivudine in human T-lymphotropic virus type-l-associated myelopathy: A randomised trial. Retrovirology **2006**; 3:63.
9. Macchi B, Balestrieri E, Ascolani A, et al. Susceptibility of primary HTLV-1 isolates from patients with HTLV-1-associated myelopathy to reverse transcriptase inhibitors. Viruses **2011**; 3:469–83.
10. De Clercq E. A cutting-edge view on the current state of antiviral drug development. Med Res Rev **2013**; 33:1249–77.
11. Wattel E, Vartanian JP, Pannetier C, Wain-Hobson S. Clonal expansion of human T-cell leukemia virus type I-infected cells in asymptomatic and symptomatic carriers without malignancy. J Virol **1995**; 69:2863–8.
12. Cavrois M, Leclercq I, Gout O, Gessain A, Wain-Hobson S, Wattel E. Persistent oligoclonal expansion of human T-cell leukemia virus type 1-infected circulating cells in patients with tropical spastic paraparesis/HTLV-1 associated myelopathy. Oncogene **1998**; 17:77–82.
13. Ishida T, Joh T, Uike N, et al. Defucosylated anti-CCR4 monoclonal antibody (KW-0761) for relapsed adult T-cell leukemia-lymphoma: a multicenter phase II study. J Clin Oncol **2012**; 30:837–42.
14. Ishida T, Utsunomiya A, Iida S, et al. Clinical significance of CCR4 expression in adult T-cell leukemia/lymphoma: its close association with skin involvement and unfavorable outcome. Clin Cancer Res **2003**; 9:3625–34.
15. Niwa R, Shoji-Hosaka E, Sakurada M, et al. Defucosylated chimeric anti-CC chemokine receptor 4 IgG1 with enhanced antibody-dependent cellular cytotoxicity shows potent therapeutic activity to T-cell leukemia and lymphoma. Cancer Res **2004**; 64:2127–33.
16. Ishii T, Ishida T, Utsunomiya A, et al. Defucosylated humanized anti-CCR4 monoclonal antibody KW-0761 as a novel immunotherapeutic agent for adult T-cell leukemia/lymphoma. Clin Cancer Res **2010**; 16:1520–31.
17. Yamano Y, Araya N, Sato T, et al. Abnormally high levels of virus-infected IFN-γ+CCR4+CD4+CD25+ T cells in a retrovirus-associated neuroinflammatory disorder. PLoS One **2009**; 4:e6517.
18. Araya N, Sato T, Ando H, et al. HTLV-1 induces a Th1-like state in CD4+CCR4+ T cells. J Clin Invest **2014**; 124:3431–42.
19. Nagai M, Brennan MB, Sakai JA, Mora CA, Jacobson S. CD8(+) T cells are an in vivo reservoir for human T-cell lymphotropic virus type I. Blood **2001**; 98:1858–61.
20. Inaoki M, Sato S, Shirasaki F, Mukaida N, Takehara K. The frequency of type 2 CD8+ T cells is increased in peripheral blood from patients with psoriasis vulgaris. J Clin Immunol **2003**; 23:269–78.
21. Cho BA, Sim JH, Park JA, et al. Characterization of effector memory CD8+ T cells in the synovial fluid of rheumatoid arthritis. J Clin Immunol **2012**; 32:709–20.
22. Hieshima K, Nagakubo D, Nakayama T, Shirakawa A, Jin Z, Yoshie O. Tax-inducible production of CC chemokine ligand 22 by human T cell leukemia virus type 1 (HTLV-1)-infected T cells promotes preferential transmission of HTLV-1 to CCR4-expressing CD4+ T cells. J Immunol **2008**; 180:931–9.
23. Osame M. Review of WHO Kagoshima meeting and diagnostic guidelines for HAM/TSP. In: Blattner WA, ed. Human retrovirology: HTLV. New York: Raven Press, **1990**: 191–7.
24. Yamano Y, Nagai M, Brennan M, et al. Correlation of human T-cell lymphotropic virus type 1 (HTLV-1) mRNA with proviral DNA load, virus-specific CD8+ T cells, and disease severity in HTLV-1-associated myelopathy (HAM/TSP). Blood **2002**; 99:88–94.
25. Lee B, Tanaka Y, Tozawa H. Monoclonal antibody defining tax protein of human T-cell leukemia virus type-I. Tohoku J Exp Med **1989**; 157:1–11.
26. Itoyama Y, Minato S, Kira J, et al. Spontaneous proliferation of peripheral blood lymphocytes increased in patients with HTLV-I-associated myelopathy. Neurology **1988**; 38:1302–7.

27. Tanner A, Bochner F, Caffin J, Halliday J, Powell L. Dose-dependent prednisolone kinetics. Clin Pharmacol Ther **1979**; 25:571–8.
28. Toulza F, Heaps A, Tanaka Y, Taylor GP, Bangham CR. High frequency of CD4+FoxP3+ cells in HTLV-1 infection: inverse correlation with HTLV-1-specific CTL response. Blood **2008**; 111:5047–53.
29. Shimizu Y, Takamori A, Utsunomiya A, et al. Impaired Tax-specific T-cell responses with insufficient control of HTLV-1 in a subgroup of individuals at asymptomatic and smoldering stages. Cancer Sci **2009**; 100:481–9.
30. Ando H, Sato T, Tomaru U, et al. Positive feedback loop via astrocytes causes chronic inflammation in virus-associated myelopathy. Brain **2013**; 136:2876–87.
31. Machigashira K, Ijichi S, Nagai M, Yamano Y, Hall WW, Osame M. In vitro virus propagation and high cellular responsiveness to the infected cells in patients with HTLV-I-associated myelopathy (HAM/TSP). J Neurol Sci **1997**; 149:141–5.
32. Sakai JA, Nagai M, Brennan MB, Mora CA, Jacobson S. In vitro spontaneous lymphoproliferation in patients with human T-cell lymphotropic virus type I-associated neurologic disease: predominant expansion of CD8+ T cells. Blood **2001**; 98:1506–11.
33. Nagai M, Usuku K, Matsumoto W, et al. Analysis of HTLV-I proviral load in 202 HAM/TSP patients and 243 asymptomatic HTLV-I carriers: high proviral load strongly predisposes to HAM/TSP. J Neurovirol **1998**; 4:586–93.
34. Iwanaga M, Watanabe T, Utsunomiya A, et al. Human T-cell leukemia virus type I (HTLV-1) proviral load and disease progression in asymptomatic HTLV-1 carriers: a nationwide prospective study in Japan. Blood **2010**; 116:1211–9.
35. Geginat J, Lanzavecchia A, Sallusto F. Proliferation and differentiation potential of human CD8+ memory T-cell subsets in response to antigen or homeostatic cytokines. Blood **2003**; 101:4260–6.
36. Kondo T, Takiguchi M. Human memory CCR4+CD8+ T cell subset has the ability to produce multiple cytokines. Int Immunol **2009**; 21: 523–32.
37. Baek HJ, Zhang L, Jarvis LB, Gaston JS. Increased IL-4+ CD8+ T cells in peripheral blood and autoreactive CD8+ T cell lines of patients with inflammatory arthritis. Rheumatology (Oxford) **2008**; 47:795–803.
38. Nagai M, Kubota R, Greten TF, Schneck JP, Leist TP, Jacobson S. Increased activated human T cell lymphotropic virus Type I (HTLV-I) Tax11–19-specific memory and effector CD8+ cells in patients with HTLV-I-associated myelopathy/tropical spastic paraparesis: correlation with HTLV-I provirus load. J Infect Dis **2001**; 183:197–205.
39. Yasunaga J, Sakai T, Nosaka K, et al. Impaired production of naive T lymphocytes in human T-cell leukemia virus type I-infected individuals: its implications in the immunodeficient state. Blood **2001**; 97:3177–83.
40. Joshi NS, Cui W, Chandele A, et al. Inflammation directs memory precursor and short-lived effector CD8+ T cell fates via the graded expression of T-bet transcription factor. Immunity **2007**; 27:281–95.
41. Kannagi M, Hasegawa A, Kinpara S, Shimizu Y, Takamori A, Utsunomiya A. Double control systems for human T-cell leukemia virus type 1 by innate and acquired immunity. Cancer Sci **2011**; 102:670–6.
42. Hanon E, Hall S, Taylor GP, et al. Abundant tax protein expression in CD4+ T cells infected with human T-cell lymphotropic virus type I (HTLV-I) is prevented by cytotoxic T lymphocytes. Blood **2000**; 95: 1386–92.
43. Vine AM, Heaps AG, Kaftantzi L, et al. The role of CTLs in persistent viral infection: cytolytic gene expression in CD8+ lymphocytes distinguishes between individuals with a high or low proviral load of human T cell lymphotropic virus type 1. J Immunol **2004**; 173:5121–9.
44. Hanon E, Stinchcombe JC, Saito M, et al. Fratricide among CD8+ T lymphocytes naturally infected with human T cell lymphotropic virus type I. Immunity **2000**; 13:657–64.
45. Sugiyama D, Nishikawa H, Maeda Y, et al. Anti-CCR4 mAb selectively depletes effector-type FoxP3+CD4+ regulatory T cells, evoking antitumor immune responses in humans. Proc Natl Acad Sci U S A **2013**; 110:17945–50.
46. Ishida T, Ueda R. Immunopathogenesis of lymphoma: focus on CCR4. Cancer Sci **2011**; 102:44–50.

ANNALS of Clinical and Translational Neurology
Open Access
AMERICAN NEUROLOGICAL ASSOCIATION since 1875

RESEARCH ARTICLE

A plasma diagnostic model of human T-cell leukemia virus-1 associated myelopathy

Makoto Ishihara[1], Natsumi Araya[2], Tomoo Sato[2], Naomi Saichi[1], Risa Fujii[1], Yoshihisa Yamano[2] & Koji Ueda[1]

[1]Division of Biosciences, Functional Proteomics Center, Graduate School of Frontier Sciences, The University of Tokyo, Tokyo, Japan
[2]Department of Rare Diseases Research, Institute of Medical Science, St. Marianna University School of Medicine, Kawasaki, Japan

Correspondence
Koji Ueda, Division of Biosciences, Functional Proteomics Center, Graduate School of Frontier Sciences, The University of Tokyo, CREST hall 1F, Institute of Medical Science, 4-6-1 Shirokanedai, Minato-ku, Tokyo, Japan, 108-8639. Tel: +81-3-6409-2062; Fax: +81-3-6409-2063; E-mail: k-ueda@ims.u-tokyo.ac.jp

Funding Information
This work was supported by grant-in-aid for Research Project on Overcoming Intractable Diseases from the Ministry of Health Labour and Welfare Japan and grant-in-aid for Young Scientists (B) (23701090) from the Ministry of Education, Culture, Sports, Science & Technology Japan.

Received: 19 November 2014; Accepted: 9 December 2014

Annals of Clinical and Translational Neurology **2015; 2(3): 231–240**

doi: 10.1002/acn3.169

Abstract

Objective: Human T-cell leukemia virus-1 (HTLV-1) associated myelopathy/tropic spastic paraparesis (HAM/TSP) is induced by chronic inflammation in spinal cord due to HTLV-1 infection. Cerebrospinal fluid (CSF) neopterin or proviral load are clinically measured as disease grading biomarkers, however, they are not exactly specific to HAM/TSP. Therefore, we aimed to identify HAM/TSP-specific biomarker molecules and establish a novel less-invasive plasma diagnostic model for HAM/TSP. **Methods**: Proteome-wide quantitative profiling of CSFs from six asymptomatic HTLV-1 carriers (AC) and 51 HAM/TSP patients was performed. Fourteen severity grade biomarker proteins were further examined plasma enzyme-linked immunosorbent assay (ELISA) assays (n = 71). Finally, we constructed three-factor logistic regression model and evaluated the diagnostic power using 105 plasma samples. **Results**: Quantitative analysis for 1871 nonredundant CSF proteins identified from 57 individuals defined 14 CSF proteins showing significant correlation with Osame's motor disability score (OMDS). Subsequent ELISA experiments using 71 plasma specimens confirmed secreted protein acidic and rich in cysteine (SPARC) and vascular cell adhesion molecule-1 (VCAM-1) demonstrated the same correlations in plasma (R = −0.373 and R = 0.431, respectively). In this training set, we constructed a HAM/TSP diagnostic model using SPARC, VCAM1, and viral load. Sensitivity and specificity to diagnose HAM/TSP patients from AC (AC vs. OMDS 1–11) were 85.3% and 81.1%, respectively. Importantly, this model could be also useful for determination of therapeutic intervention point (OMDS 1–3 + AC vs. OMDS 4–11), exhibiting 80.0% sensitivity and 82.9% specificity. **Interpretation**: We propose a novel less-invasive diagnostic model for early detection and clinical stratification of HAM/TSP.

Introduction

The RNA retrovirus human T-cell leukemia virus-1 (HTLV-1) is endemic in Japan, Caribbean basin, Iran, Africa, South America, and the Melanesian islands.[1] Number of infected individuals is currently estimated at around 30 million worldwide,[2] in which 5% of virus carriers develop HTLV-1 associated myelopathy/tropic spastic paraparesis (HAM/TSP) or adult T-cell leukemia (ATL) after asymptomatic phase of typically over 30 years. Inflammation of spinal cord is a principal symptom of HAM/TSP patients, causing progressive scelotyrbe, gait impairment, or urination disorder.[3] However, no curative therapy for HAM/TSP has been developed except for anti-inflammatory treatments by INF-α or steroids,[4] whereas excessive or long-term use of these drugs can increase the risk of adverse events.[5,6] Hence, the treatment regimens should be carefully managed based on a thorough assessment of disease stage and activity. As for the severity grading of HAM/TSP, Osame's motor disability score (OMDS) is widely used to define disease stages and estimate the rate of disease progression.[7] Although this scale is helpful to evaluate consequential impairment of motor functions, development of molecular-based

diagnostics has been a major challenge for early detection and adequate therapeutic intervention of HAM/TSP.

To identify HAM/TSP-specific biomarkers, a variety of genomic or proteomic analyses were performed for infected T cells and plasma samples,[8-10] however, comprehensive investigation for cerebrospinal fluid (CSF) has not been launched in spite of the most fundamental site of HAM/TSP lesion. Therefore, we intended to acquire the first proteome-wide view of CSFs reflecting HAM/TSP-associated alteration of spinal cord microenvironment. Following the statistical identification of severity grade biomarkers from CSFs, we attempted to construct a HAM/TSP diagnostic model using less-invasive plasma specimens.

Subjects and Methods

Participants

CSF specimens (from 51 HAM/TSP patients and six asymptomatic carriers [ACs]) and plasma specimens (from 50 HAM/TSP patients and 55 ACs) were collected in St. Marianna University School of Medicine and kept frozen at −80°C until just before use. The research procedure was explained and written informed consent was obtained from all the patients. This study was approved by the Ethical Committee of the University of Tokyo (approval code 14-1) and the Ethical Committee of St. Marianna University School of Medicine.

LC/MS/MS analysis

The 20 μL each of CSFs was lyophilized and dissolved in 8 mol/L Urea (GE Healthcare, Buckinghamshire, UK) in 50 mmol/L ammonium bicarbonate (Sigma-Aldrich, St. Louis, MO). After reduction with 5 mmol/L tris(2-carboxyethyl)phosphine (Sigma-Aldrich) at 37°C for 30 min, proteins were alkylated with 25 mmol/L Iodoacetamide (Sigma-Aldrich) at ambient temperature for 45 min. Following fourfold dilution with 50 mmol/L ammonium bicarbonate, proteins were digested with immobilized trypsin (Thermo Scientific, Bremen, Germany) at 37°C for 6 h. Digested samples were then desalted by Oasis HLB μElution plate (Waters, Milford, MA) and analyzed by liquid chromatography - tandem mass spectrometry (LC/MS/MS). The peptides were separated on Ultimate 3000 RSLC nano-HPLC system (Thermo Scientific) equipped with 0.075 × 150 mm C_{18} tip-column (Nikkyo Technos, Tokyo, Japan) using two-step linear gradient comprising 2–35% acetonitrile for 95 min and 35–95% acetonitrile for 15 min in 0.1% formic acid at the flow rate of 250 nL/min. The eluates were analyzed with LTQ Orbitrap Velos mass spectrometer (Thermo Scientific). Spectra were collected using full MS scan mode over the mass-to-charge (*m/z*) range 400–1600. MS/MS was performed on the top 20 ions in each MS scan using the data-dependent acquisition mode with dynamic exclusion enabled.

2D-LC/MS/MS analysis

CSF tryptic digests were resolved in 10 mmol/L ammonium formate (Sigma-Aldrich) in 25% acetonitrile and fractionated with 0.2 × 250 mm strong cation exchange monolith column (GL Science, Tokyo, Japan). The samples were eluted with the gradient from 10 mmol/L to 1 mol/L of ammonium formate in curve = 3 mode within 70 min using Prominence HPLC system (Shimadzu Corporation, Kyoto, Japan). The eluate was separated into 11 fractions and analyzed by LC/MS/MS.

Protein/peptide identification

MS/MS spectra were searched against SwissProt database version 2012_06 (20,232 human protein sequences) using SEQUEST algorithm on ProteomeDiscoverer 1.3 software (Thermo Scientific). Proteins satisfying the false discovery rate (FDR) <1% by Peptide Validator FDR estimation algorithm on ProteomeDiscoverer was accepted. Gene ontology (GO) term analysis was performed using DAVID Bioinformatics Resources 6.7 (http://david.abcc.ncifcrf.gov/).

Label-free quantification analysis

The LC/MS/MS data from 57 CSF samples were imported on the Expressionist server (Genedata AG, Basel, Swiss) and processed along the workflow shown in Figure S1. The four-step Chromatogram Chemical Noise Subtraction was performed, composed of (1) RT structure removal = true, minimum RT length = 2 scans, (2) *m/z* structure removal = true, minimum *m/z* length = 6 scans, (3) RT window = 501 scans, quantile subtraction = 90%, and (4) RT structural removal = true, minimum RT length = 2 scans. Data points with intensity <500 were clipped to zero. Again, Chromatogram Chemical Noise Subtraction was performed using chromatogram smoothing = true, RT windows = 5 scans, and estimator = Moving average. After applying Chromatogram Grid with a distance of scan counts = 10, RT variety among 57 samples was normalized by Chromatogram RT Alignment: *m/z* windows = 11 points, RT windows = 11 scans, gap penalty = 1, RT search interval = 2 min, alignment scheme = pairwise alignment based tree. Peaks were detected by Chromatogram Summed Peak Detection: summation window = 20 scans, overlap = 10, minimum peak size = 6 scans, maximum merge distance = 1 point,

peak RT splitting = true, intensity profiling = maximum, gap/peak ratio = 5%, refinement threshold = 80, consistency threshold = 1. The detected peaks were grouped in isotopic clusters using Chromatogram Isotopic Peak Clustering: minimum charge = 1, maximum charge = 10, maximum missing peaks = 0, first allowed gap position = 10, RT window = 0.02 min, *m/z* tolerance = 5 ppm, isotope shape tolerance = 10, minimum cluster size ration = 0.5.

Cytometric bead array

Concentration of C-X-C motif chemokine 10 (CXCL10) in CSF was determined by cytometric bead array (CBA) (BD Biosciences, San Jose, CA) according to the manufacturer's instructions.

Enzyme-linked immunosorbent assay

Concentrations of secreted protein acidic and rich in cysteine (SPARC) (R&D Systems, Minneapolis, MN) and vascular cell adhesion molecule-1 (VCAM1) (Abcam, Cambridge, MA) in 105 plasma samples were measured with commercial enzyme-linked immunosorbent assay (ELISA) kit following the manufacturer's instructions. A multivariate logistic regression was applied to construct a new diagnostic model for HAM/TSP utilizing three factors, SPARC, VCAM1, and viral load, as described previously.[11]

Result

Quantitative proteome profiling of CSFs from HAM/TSP patients

CSFs from 6 ACs and 51 HAM/TSP patients (Table 1) were processed according to the schematic workflow of this study (Fig. 1). Nonredundant 68,077 peptides from 57 individuals were detected and quantified on the Expressionist proteome server system, meanwhile 14,451

Table 1. Clinical characteristics of the CSF specimens.

Group	*N*	Age (±SD)	Gender (M/F)
AC	6	55.7 (±15.8)	4/2
HAM1_3	7	57.9 (±14.2)	3/4
HAM4_6	35	59.3 (±11.0)	11/24
HAM7_11	9	61.6 (±8.0)	1/8
Total	57	59.1 (±11.7)	19/38

CSF, cerebrospinal fluid; AC, asymptomatic carriers; HAM1_3, HAM/TSP patients whose Osame's motor disability score from 1 to 3; HAM4_6, HAM/TSP patients whose Osame's motor disability score from 4 to 6; HAM7_11, HAM/TSP patients whose Osame's motor disability score from 7 to 11.

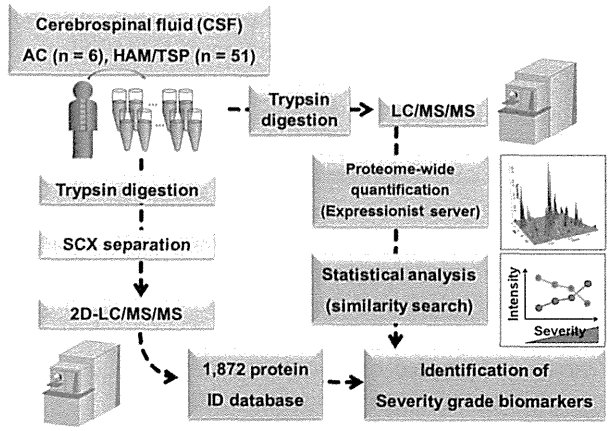

Figure 1. Schematic overview of severity grade marker screening. Cerebrospinal fluids (CSFs) from six asymptomatic carriers (ACs) and 51 HAM/TSP patients were analyzed by LC/MS/MS. Candidate peptides whose intensities had correlation with severity grades were isolated according to Pearson product-moment correlation coefficient. Candidate peptides were identified using Protein/Peptide identification database established by 2D-LC/MS/MS. HAM/TSP, human T-cell leukemia virus-1 associated myelopathy/tropic spastic paraparesis.

CSF peptides (1871 proteins) were identified by parallel 2D-LC/MS/MS analysis. To evaluate quantitative reliability of our LC/MS-based proteome profiling, observed relative concentrations of CXCL10 (Interferon gamma Inducible protein 10, CXCL10) were compared to clinical data which were measured by CBA (Fig. 2A). The result showed strong correlation (R^2 = 0.911) between two measurements, indicating that our LC/MS-based quantification results were highly credible even in the low concentration range (1–20 ng/mL).

Next, to interpret proteome-wide alterations in CSF environment of HAM/TSP patients, 1345 or 1750 proteins identified from AC or HAM/TSP patients group, respectively (Fig. 2B), were classified according to cellular component (CC, Fig. 2C and D) or biological process (BP, Fig. 2E and F) using DAVID Functional Annotation Tool. The CC analysis revealed that proteins expressed in cell projection and plasma membrane were enriched in CSF of HAM/TSP patients, in addition to specific enrichment of viral proteins. This may reflect increased invasive activity of HTLV-1-infected cells into spinal cord, which is often observed in HAM/TSP patients. Further BP analysis indicated that proteins involved in cell adhesion, cell motion, cell migration, cytoskeleton, and cell structure disassembly were highly enriched in CSF of HAM/TSP patients. These features also denoted proteome-wide environmental change in spinal cord, inducing active migration and/or invasion of lymphocytes. Proteins related to cell death and cell growth might associate with spinal inflammation in HAM/TSP patients.

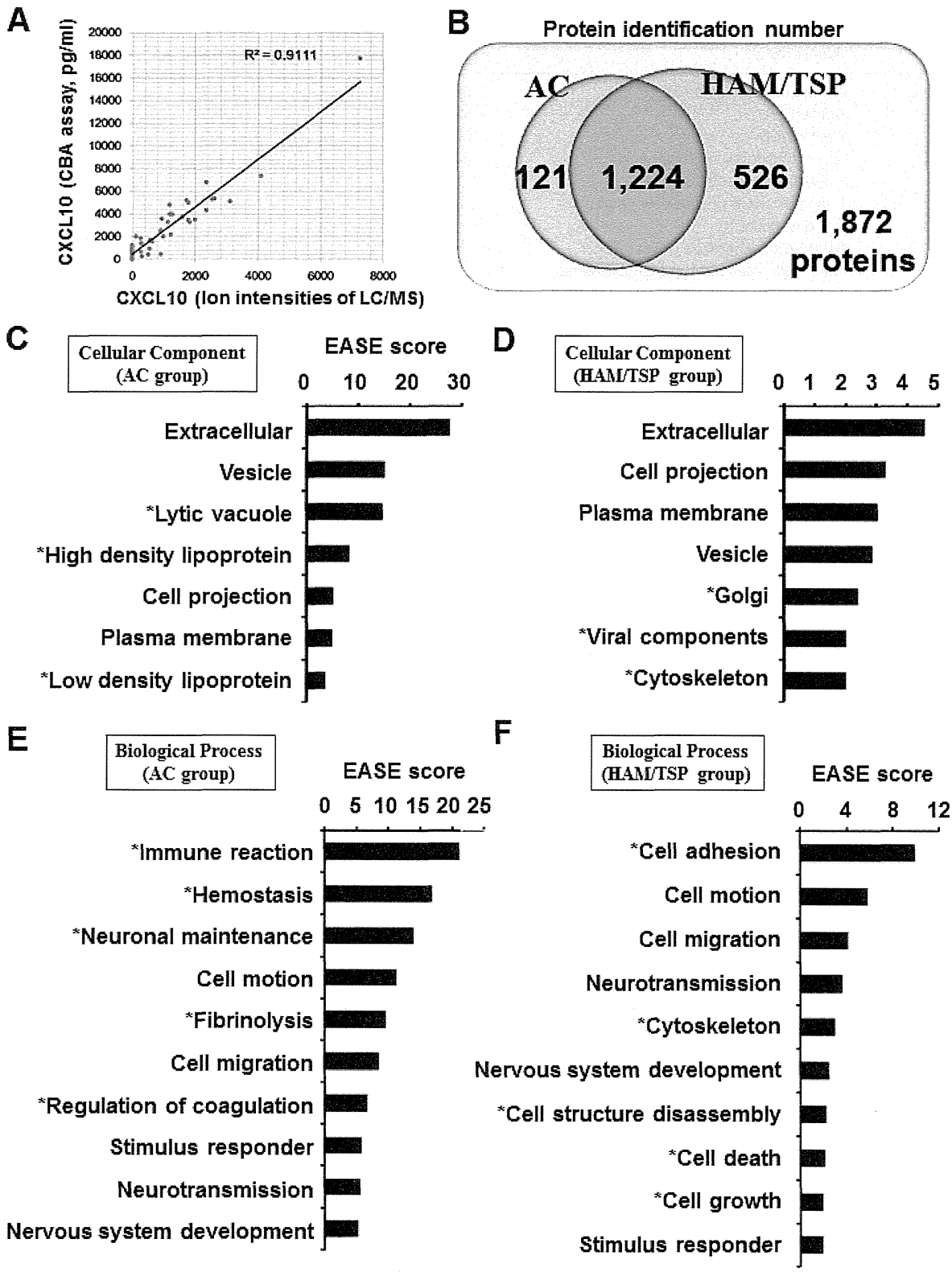

Table 2. List of 16 severity grade markers for HAM/TSP.

UniProt accession	Protein name	Amino acid numbers of identified peptide	Pearson's correlation coefficient (*R*)	*P*-value
Q9NZK5	Adenosine deaminase CECR1	247–258	0.478	5.15E-04
Q12860	Contactin-1	634–647	−0.425	9.94E-04
Q14118	Dystroglycan	222–232	−0.463	2.89E-04
Q8N2S1	Latent-transforming growth factor beta-binding protein 4	310–323	−0.463	2.90E-04
Q9Y5Y7	Lymphatic vessel endothelial hyaluronic acid receptor 1	8–18	−0.499	9.15E-05
Q16653	Myelin-oligodendrocyte glycoprotein	14–25	−0.444	5.40E-04
Q9UJJ9	N-acetylglucosamine-1-phosphotransferase subunit gamma	47–56	−0.442	5.72E-04
P13591	Neural cell adhesion molecule 1	586–597	−0.459	3.31E-04
P36955	Pigment epithelium-derived factor	133–141	−0.454	3.83E-04
Q9UHG2	ProSAAS	14–24	−0.444	5.42E-04
P09486	Secreted protein acidic and rich in cysteine	124–133	−0.523	3.01E-05
P09486	Secreted protein acidic and rich in cysteine	156–164	−0.477	1.75E-04
P09486	Secreted protein acidic and rich in cysteine	252–262	−0.457	3.55E-04
Q92563	Testican-2	139–148	−0.424	1.03E-03
Q06418	Tyrosine-protein kinase receptor TYRO3	279–290	−0.438	1.04E-03
P19320	Vascular cell adhesion protein 1	581–590	0.430	9.35E-04

HAM/TSP, human T-cell leukemia virus-1 associated myelopathy/tropic spastic paraparesis.

Statistical analysis for screening severity grade marker candidates

To extract biomarker proteins showing stoichiometric increase/decrease in accordance with progression of HAM/TSP, numerical classes (0, 1, 2, and 3) were given to four clinically relevant severity groups (AC, HAM/TSP OMDS 1–3, 4–6, and 7–11, respectively) (see Table S1). Then quantitative correlation between severity classes and 68,077 peptide intensities was ranked with Pearson's correlation analysis. Peptides with the lowest 100 *P*-values (Table S2) were next subjected to protein identification analysis by 2D-LC/MS/MS, resulting in successful identification of 14 proteins derived from 16 peptides (Table 2). In addition to Pearson's correlation coefficients and *P*-values in Table 2, LC/MS-based quantitative profiles of 16 peptides were illustrated with box plots (Fig. 3). Compared to a traditional severity grade marker neopterin ($R = 0.4105$, $P = 1.12E\text{-}03$), any of identified proteins showed better potential to be utilized as CSF disease state biomarkers.

SPARC and VCAM-1 as HAM/TSP severity grade markers in plasma

To further narrow down the biomarker candidates and establish plasma-based less-invasive diagnostics, we examined plasma levels of the 14 proteins by ELISA assays measuring 71 training cases (Table 3). The results revealed that a couple of proteins, SPARC and VCAM1, showed the same correlation in plasma with CSF levels ($|R| > 0.4$ and $P < 0.05$) (Fig. 4A and B). Therefore, we attempted construction of the combination biomarker diagnostics using newly identified two proteins and HTLV-1 viral load, all of which are measurable from small volume of blood samples. In order to halt the progression of HAM/TSP and maintain better quality of life for patients, both early diagnosis of HAM/TSP onset and therapeutic intervention at appropriate time point are essential. On the basis of these clinical requirements, we made two logistic regression models which maximized area under the curve (AUC) of ROC curves comparing ACs with HAM/TSP patients (onset predictor; (1)) or

Figure 2. Summary of CSF proteome. (A) Evaluation of LC/MS-based quantification analysis. The relative concentrations of CXCL10 cytokine calculated by mass spectrometric analysis were compared to independent measurements by cytometric bead array (CBA). (B) Venn diagram of identified proteins in 57 CSF analyses. The Gene Ontology (GO) analysis using DAVID Bioinformatics Resources displayed enriched cellular components of CSF proteins in ACs (C) or HAM/TSP patients (D). The enriched biological functions of CSF proteins in ACs (E) or HAM/TSP patients (F) were also shown. Expression Analysis Systematic Explorer (EASE) enrichment scores were shown. CSF, cerebrospinal fluid; CXCL10, C-X-C motif chemokine 10; ACs, asymptomatic carriers; HAM/TSP, human T-cell leukemia virus-1 associated myelopathy/tropic spastic paraparesis.

